DOI 10.1002/pmic.200401300 *Proteomics* 2005, *5,* 2908–2926

REGULAR ARTICLE

Proteomic analysis of redox- and ErbB2-dependent changes in mammary luminal epithelial cells using cysteine- and lysine-labelling two-dimensional difference gel electrophoresis

Hong-Lin Chan[1], Severine Gharbi[1], Piers R. Gaffney[2], Rainer Cramer[1], Michael D. Waterfield[1] and John F. Timms[1]

[1] Ludwig Institute for Cancer Research and Department of Biochemistry and Molecular Biology University College London, London, UK
[2] Department of Chemistry, Imperial College, London, UK

Received: August 9, 2004
Revised: February 22, 2005
Accepted: February 23, 2005

Differential protein expression analysis based on modification of selected amino acids with labelling reagents has become the major method of choice for quantitative proteomics. One such methodology, two-dimensional difference gel electrophoresis (2-D DIGE), uses a matched set of fluorescent *N*-hydroxysuccinimidyl (NHS) ester cyanine dyes to label lysine residues in different samples which can be run simultaneously on the same gels. Here we report the use of iodoacetylated cyanine (ICy) dyes (for labelling of cysteine thiols, for 2-D DIGE-based redox proteomics. Characterisation of ICy dye labelling in relation to its stoichiometry, sensitivity and specificity is described, as well as comparison of ICy dye with NHS-Cy dye labelling and several protein staining methods. We have optimised conditions for labelling of nonreduced, denatured samples and report increased sensitivity for a subset of thiol-containing proteins, allowing accurate monitoring of redox-dependent thiol modifications and expression changes. Cysteine labelling was then combined with lysine labelling in a multiplex 2-D DIGE proteomic study of redox-dependent and ErbB2-dependent changes in epithelial cells exposed to oxidative stress. This study identifies differentially modified proteins involved in cellular redox regulation, protein folding, proliferative suppression, glycolysis and cytoskeletal organisation, revealing the complexity of the response to oxidative stress and the impact that overexpression of ErbB2 has on this response.

Keywords:
Breast cancer / Chaperones / ErbB2 / Mass spectrometry / Peroxiredoxins / Redox proteomics / Thiol-reactive cyanine dyes / Two-dimensional difference gel electrophoresis

Correspondence: Dr. John F. Timms, Ludwig Institute for Cancer Research and Department of Biochemistry and Molecular Biology University College London, Cruciform Building, Gower Street, London WC1E 6BT, UK
E-mail: jtimms@ludwig.ucl.ac.uk
Fax: +44-207-679-6334

Abbreviations: AmBic, ammonium bicarbonate; **BVA**, biological variation analysis; **α-Crys**, α-crystallin; **Cy2**, 3-(4-carboxymethyl)phenylmethyl-3′-ethyloxacarbocyanine halide; **Cy3**, 1-(5-carboxypentyl)-1′-propylindocarbocyanine halide; **Cy5**, 1-(5-carboxypentyl)-1′-methylindocarbocyanine halide; **ddH_2O**, double deionised water; **DIA**, difference in-gel analysis; **G3PDH**, glyceraldehyde 3-phosphate dehydrogenase; **HMLECs**, human mammary luminal epithelial cells; **H_2O_2**, hydrogen peroxide; **Hsp**, heat-shock protein; **5-IAF**, 5-iodoacetamidofluorescein; **IAM**, iodoacetamide; **ICy**, iodoacetylated cyanine dye; **Myo**, myoglobin; **NHS**, *N*-hydroxysuccinimidyl; **Ova**, ovalbumin; **Prxn**, peroxiredoxin; **RhoGDI1**, Rho-GDP-dissociation inhibitor 1; **TBS-T**, Tris buffered saline-Tween-20; **TCP**, T-complex protein; **TPI**, triosephosphate isomerase; **UPR**, unfolded protein response

1 Introduction

2-DE is one of the most widely used proteomic separation methods for the analysis of differential protein expression in biological samples [1, 2]. However, as most users realise, 2-DE and some of the methods commonly used for in-gel protein visualisation (such as silver staining) are inherently variable and many replicate gels must be run before significant differences in protein expression can be ascribed with accuracy. Moreover, the protein visualisation methods used often have narrow linear dynamic ranges of detection, making them unsuitable for the analysis of biological samples where protein copy numbers vary enormously. A significant improvement in the ability to use gel-based methods for protein quantitation and detection was achieved with the introduction of 2-D DIGE, which enables codetection of several samples on the same 2-DE gel, so minimising gel-to-gel variation [3–5]. This is accomplished by the differential covalent modification of proteins with spectrally distinct, but charge- and size-matched fluorescent dyes, prior to electrophoretic separation.

The original 2-D DIGE methodology uses three *N*-hydroxysuccinimidyl (NHS) ester-derivatives of the cyanine dyes (NHS-3-(4-carboxymethyl)phenylmethyl-3'-ethyloxacarbocyanine halide (Cy2), NHS-1-(5-carboxypentyl)-1'-propylindocarbocyanine halide (Cy3) and NHS-1-(5-carboxypentyl)-1'-methylindocarbocyanine halide (Cy5)), for labelling of protein primary amino groups (*i.e.* lysine ε-amino and *N*-terminal α-amino groups). Such Cy-labelled samples are mixed and separated on the same 2-DE gel and so the samples being compared are subjected to identical procedures and microenvironments during the gel running. This allows the generation of directly superimposable 2-DE images for each sample, which are valid over the wider linear dynamic range afforded by fluorescence detection. Ideally for 2-D DIGE expression profiling, one dye (*e.g.* Cy2) is used to label an internal standard (consisting of an equal pool of all samples) which is run on every gel against the Cy3- and Cy5-labelled test samples [3, 6]. The fluorescence signal from each protein feature (Cy3- or Cy5-labelled) is then compared with the comigrating standard feature (Cy2-labelled) on each gel to give a standardised abundance ratio that can be averaged across replicate samples and compared between different samples to allow identification of significant changes. This strategy provides improved accuracy in quantifying protein differences between samples and eliminates experimental variation due to potential dye-labelling bias. Cy dye lysine labelling is typically carried out under conditions that limit modification to an estimated 3–5% of total protein; so-called 'minimal' labelling [4]. This low stoichiometry labelling is necessary to avoid sample insolubility and heterogeneous multiple labelling which would complicate image analysis and spot picking by introducing spot trains in the molecular weight dimension. Overlabelling of lysine may also block tryptic cleavage sites, hindering the downstream identification of labelled proteins by MS.

To improve the sensitivity of the technique and facilitate protein spot identification, it would be preferable to label a less prevalent amino acid at higher stoichiometry such as cysteine, which can be labelled through alkylation of its thiol group and is not a cleavage site for the proteases commonly used in peptide mass mapping. With this in mind, GE Healthcare recently commercialised a pair of maleimide Cy dyes for cysteine thiol saturation labelling of reduced and denatured samples. Evaluation of this strategy showed improved sensitivity and dynamic range over minimal labelling, and combines the higher accuracy afforded by DIGE differential labelling [7]. This strategy was recently applied in two separate studies to identify proteomic changes in rare samples; between laser microdissected normal intestinal epithelium and adenoma [8] and between differentially sorted murine bone marrow cell populations displaying distinct chemotactic responses [9].

A further advantage of cysteine labelling is that it can be used to monitor changes in the redox status of protein thiols in response to particular stimuli, such as oxidants, growth factors or inflammatory cytokines. Since reactive oxygen species can activate signalling pathways, modulate a variety of cellular activities and seem to play an important role in disease progression, it is important to study the molecular events associated with their effects. Indeed, there have been several reports of redox proteomic strategies using fluorescent or radio-labelled alkylating agents to detect thiol-containing protein in gels. For example, Baty *et al.* [10] developed a method to monitor reduction and oxidation of protein thiols by blocking reduced thiols with *N*-ethylmaleimide followed by reduction of oxidised thiol proteins with DTT prior to labelling with 5-iodoacetamidofluorescein (5-IAF) and analysis by 2-DE. Application of this method to examine the effect of diamide treatment on Jurkat cells showed a dramatic increase in thiol protein oxidation after treatment, with few detectable changes in reduced thiol proteins. Similarly, 5-IAF labelling and antifluorescein immunoblotting were used to detect intracellular hydrogen peroxide (H_2O_2)-sensitive proteins [11], whilst the same group used radioactive iodoacetic acid to show that protein tyrosine phosphatase PTP1B is reversibly oxidised by growth factor-induced intracellular H_2O_2 [12]. Finally, a Cy5 maleimide dye labelling strategy was used to detect thioredoxin-targeted proteins in barley seeds [13]. Although these studies show the usefulness of thiol labelling to examine redox-associated events, gel-to-gel variation is still a problem and it would be preferable to apply cysteine-labelling 2-D DIGE to improve the accuracy in such sample comparisons.

With this purpose in mind we synthesised a pair of thiol-reactive iodoacetyl derivatives of Cy3 and Cy5 (termed ICy3 and ICy5) and developed a cysteine-labelling strategy for 2-D DIGE-based expression and redox proteomics. The present study describes the characterisation and optimisation of ICy dye labelling using standard proteins and cell lysates. We have examined labelling stoichiometry, sensitivity and specificity and compared the ICy dye technique with conventional

NHS-Cy dye labelling and three MS-compatible protein staining techniques. The strategy was then applied in a multiplexed study with the NHS-Cy dyes to analyse redox-dependent changes in protein expression and thiol reactivity in a matched pair of human mammary luminal epithelial cell lines (HMLECs) expressing different levels of the ErbB2 growth factor receptor and exposed to oxidative stress. ErbB2 (Her-2/Neu) is a receptor tyrosine kinase overexpressed in 25–30% of human breast cancers, an event that is associated with poor prognosis and an increased likelihood of metastasis [14]. Despite intensive research efforts, the biological mechanisms underlying the oncogenicity of the ErbB2 receptor are still poorly understood. In addition, little is known about the cellular targets of oxidative stress, the mechanisms of cellular protection from oxidative stress or the effects of oncogene expression on redox signalling. This study was aimed at a further understanding of these processes. A number of differentially labelled proteins (redox-sensitive and ErbB2-dependent) were identified from gels by MS. Using both cysteine and lysine 2-D DIGE, we have revealed some of the players involved in the cellular response to oxidative stress and the impact that ErbB2 overexpression has on this response.

2 Materials and methods

2.1 Synthesis of Cy dyes

NHS ester derivatives of the fluorescent cyanine dyes Cy3 and Cy5 (NHS-Cy3 and NHS-Cy5) for lysine labelling were synthesised in-house following a modified version of the published protocol [5]. These dyes are structurally identical to the commercially available NHS-Cy dyes. Briefly, Cy carboxylic acids were prepared from the reactions of 1 and 2 (Fig. 1A), and these converted to the corresponding NHS-Cy reagents. To optimise yields and ensure compound purity, each of the reported intermediates for NHS-Cy preparation was purified before commencing the next step, instead of carrying through crude material. In our hands, the published preparation of 1b gave poor and variable yields; therefore an alternative preparation that has worked reliably for several phenylimido indoline Cy3 and Cy5 precursors was used (see Supplementary Material). Also, in our hands, the published preparation of 2 gave material significantly contaminated with 1-[6-hexanoyl(6-hexanoic acid)]-2-methylene-3,3-dimethyl indolinium bromide. We have overcome this by alkylating 2,3,3-trimethyl indolenine with a 6-bromohexanoate silyl ester. Iodoacetyl versions of Cy3 and Cy5 (ICy3 and ICy5) were synthesised *via* the illustrated route starting with the reaction of 1 and 3 (Fig. 1A and Supplementary Material). The structures are shown in Fig. 1B. ^{1}H and ^{13}C NMR spectra of the dyes were consistent with their being a single compound present for each of the structures shown, indicating high purity, and ESI-MS gave a single base peak with a mass consistent with the cationic form of each dye. All Cy dyes were made as stock solutions in anhydrous 99.8% *N,N*-dimethylformamide and stored at −20°C.

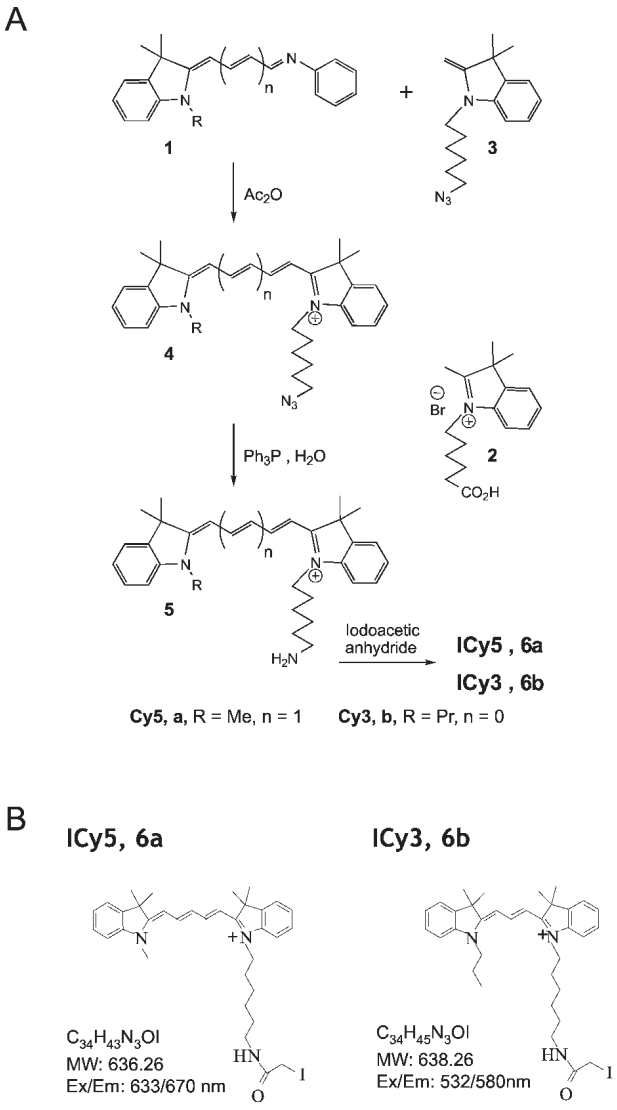

Figure 1. Synthesis and structure of the iodoacetyl cyanine dyes. (A) Scheme for synthesis of ICy3 and ICy5. A detailed description of the synthesis and purification strategy of these compounds is provided as Supplementary Material. (B) ICy5 and ICy3 (compounds 6a and 6b respectively from the synthetic scheme), showing chemical formulae, molecular weights and the excitation/emission wavelengths used for detection.

2.2 Labelling of standard proteins

Standard proteins used were BSA, chicken ovalbumin (Ova), *S. japonicum* GST, bovine α-crystallin (α-Crys) A and B chains and horse myoglobin (Myo). All proteins were from

Sigma except GST, which was expressed in *E. coli* and purified on glutathione sepharose beads according to standard procedures.

Standards were solubilised in denaturing 2-D lysis buffer (4% w/v CHAPS, 8 M urea, 10 mM Tris-HCl, pH 8.3, 1 mM EDTA) and an equimolar mixture prepared containing 2 pmol of each protein. Labelling with NHS-Cy3/5 or ICy3/5 was carried out at the indicated dye to protein ratios for 1 h on ice in the dark, after which the NHS-Cy reactions were quenched with a 20-fold molar excess of free lysine to dye for 10 min on ice. All samples were reduced with DTT at 65 mM prior to gel analysis. In some cases, samples were reduced with DTT, acetone precipitated and resolubilised prior to labelling. The number of free thiols in BSA, Ova and α-Crys was assessed using Ellman's reagent (5,5'-dithiobis-2-nitrobenzoate – DTNB). Briefly, different amounts of each standard were diluted in 2.9 mL of 10 mM sodium phosphate buffer (pH 8.0) and 100 μL of 10 mM DTNB in sodium phosphate buffer added. The mixture was left to stand in the dark for 15 min and then the absorbance measured at 412 nm against a reference solution without protein. The concentration of free thiol groups was calculated using the equation: [SH] = [A412 (sample) − A412 (reference)]/13 650.

2.3 Cell culture and peroxide treatment

The HMLEC line HB4a and its ErbB2-overexpressing derivative C3.6 have been described previously [3, 15]. Cells were maintained in RPMI-1640 medium with 10% v/v foetal calf serum, 2 mM glutamine, 100 IU/mL penicillin, 100 μg/mL streptomycin (Invitrogen), 5 μg/mL hydrocortisone and 5 μg/mL insulin (Sigma) at 37°C in a 10% CO_2 humidified incubator. For the oxidative stress study, cells in 10 cm dishes at ~80% confluence were treated with H_2O_2 at 0.5 mM final concentration by addition to the growth media. Cells were harvested after the indicated times.

2.4 Cell lysis and Cy dye labelling

Cells were washed twice in 0.5 × PBS (Invitrogen), drained well and lysed in 2-D lysis buffer (see Section 2.2) with no reductant. Samples were homogenised by passage through a 25-gauge needle (six times) and insoluble material removed by centrifugation (13 000 rpm/10 min/4°C). Protein concentration was determined using Coomassie Protein Assay Reagent (Pierce). Extracts were labelled with ICy3/5 at 80 pmol/μg protein on ice in the dark for 1 h and reactions quenched with DTT (65 mM final concentration). For NHS-Cy labelling, 4 pmol/μg of dye was used and reactions quenched with a 20-fold molar excess of lysine to dye, prior to addition of DTT. For ICy labelling, cells were lysed in the presence of dye to limit postlysis thiol modification. Since ICy dye interfered with the protein assay, protein concentrations were determined on replica lysates not containing dye. Test samples (control or H_2O_2 treated) were labelled with the same ICy dye and mixed with an equal amount of standard pool labelled with the other dye, prepared by mixing equal amounts of protein from all samples. For NHS-Cy labelling, samples were labelled with Cy3 or Cy5, and run against a standard pool labelled with Cy2. Volumes were adjusted to 350 μL with buffer plus DTT and carrier Ampholines (pH 3–10) added to 2% v/v. All samples were run in triplicate against the standard pool.

2.5 1- and 2-DE

Cy-labelled proteins in Laemmli sample buffer were separated by 1-D SDS-PAGE according to standard procedures, except that samples in urea-containing buffer were not boiled and low-fluorescence glass plates were used. For 2-DE, 18 cm, nonlinear pH 3–10 IPG strips (GE Healthcare) were rehydrated with Cy-labelled samples in the dark at room temperature overnight. IEF was performed on a Multiphor II (GE Healthcare) for 80 kVh at 20°C. Strips were equilibrated for 10 min in 50 mM Tris-HCl pH 6.8, 6 M urea, 30% v/v glycerol and 2% w/v SDS containing 65 mM DTT and then for 10 min in the same buffer containing 240 mM iodoacetamide (IAM). Equilibrated IPG strips were then transferred onto 1.5 mm thick 18 × 20 cm 12% polyacrylamide gels cast between low-fluorescence glass plates. Gels were bonded to the inner surface of one plate at casting by pretreatment with bind-silane solution (80% ethanol, 2% acetic acid, 0.08% bind-silane (PlusOne; GE Healthcare)) according to the manufacturer's protocol. Strips were overlaid with 0.5% w/v low melting point agarose in running buffer with bromophenol blue. Gels were run in Protean II tanks (Bio-Rad) at 10 mA *per* gel at 10°C until the dye front had run off the bottom. All steps were carried out in a dedicated clean room.

2.6 Detection of dye-labelled proteins

1- and 2-D gels were scanned between low-fluorescence glass plates using either a CCD-based 2920 2DMasterImager with PixCel software or a Typhoon 9400 multicolour fluorescence scanner using ImageQuant software (both from GE Healthcare). The exposure time (2920 2DMasterImager) or PMT voltage (Typhoon 9400) was adjusted on each channel (Cy2/3/5) for preliminary low resolution scans (1000 μm) to give maximum pixel values within 10% for each Cy image but below the saturation level. These settings were then used for high resolution (100 μm) scans. Images were exported as tif files for image analysis.

2.7 Image analysis

2-D images were curated and analysed using Melanie IV (Swiss Institution of Bioinformatics) and DeCyder™ (GE Healthcare), whilst 1-D images were analysed using ImageQuant software (GE Healthcare). For presentation purposes only, images were pseudocoloured and overlaid using Adobe Photoshop (Adobe Systems). For DeCyder analysis, the dif-

ference in-gel analysis (DIA) module was first used to define spot boundaries and to measure normalised spot volumes of Cy-labelled features for calculation of difference ratios for samples run on the same gel. Features resulting from non-protein sources (*e.g.* dust particles and scratches) were filtered out. The biological variation analysis (BVA) mode of DeCyder was then used to match all images for comparative cross-gel statistical analysis with user intervention required to set landmarks for accurate matching. Comparison of test spot volumes with the corresponding standard spot volumes gave a standardised abundance for each matched spot and values were averaged across triplicates for each experimental condition. Spots displaying a $\geq$1.5 average-fold increase or decrease in abundance and with p-values < 0.05 were selected for analysis.

2.8 Protein-staining

Silver and colloidal Coomassie blue G-250 staining (CCB) were used to visualise gel separated Cy dye-labelled proteins. For silver staining of nonbonded gels, a MS-compatible method was used [16]. Briefly, gels were fixed for >3 h in fix solution (40% methanol, 7.5% v/v acetic acid) and washed twice for 15 min each in double deionised water (ddH_2O). Gels were sensitised in 0.02% w/v sodium thiosulphate for 1 min, washed twice in ddH_2O for 1 min each, incubated for 30 min in 0.15% w/v silver nitrate at 4°C and washed twice in ddH_2O for 1 min each before developing in 2% w/v sodium carbonate with 0.02% v/v formaldehyde. Staining was quenched with 5% v/v acetic acid and gels stored in 1% v/v acetic acid at 4°C for spot picking and MS. For CCB staining, a modification of the protocol by Neuhoff *et al.* [17] was used. Bonded gels were fixed in 35% v/v ethanol, 2% v/v phosphoric acid for >3 h, washed 3 × 30 min in ddH_2O and incubated in 34% v/v methanol, 17% w/v ammonium sulphate, 3% v/v phosphoric acid for 1 h, prior to addition of 0.5 g/L Coomassie G-250 (Merck) and left to stain for 2–3 days. No destaining step was required. Stained gels were imaged on a Bio-Rad GS-800 densitometer (silver and CCB) or Typhoon™ 9400 scanner using the red laser and no emission filters (CCB).

2.9 Spot picking and in-gel digestion

Poststained images were matched with Cy dye images using DeCyder or Melanie IV software and a pick list of coordinates created for spots of interest relative to reference markers fixed to the glass plates at casting. Spots were excised using an Ettan automated spot picker (GE Healthcare) from gels submerged under ddH_2O. Spots were collected in 96-well plates, drained and stored at −20°C prior to MS. In some experiments, spots were picked without poststaining using coordinates from the ICy-labelled image. For in-gel digestion, gel pieces were washed three times in 50% ACN, dried in a SpeedVac for 10 min, reduced with 10 mM DTT in 5 mM ammonium bicarbonate pH 8.0 (AmBic) for 45 min at 50°C and then alkylated with 50 mM IAM in 5 mM AmBic for 1 h at 22°C in the dark. Gel pieces were then washed three times in 50% ACN and vacuum-dried before reswelling with 50 ng of modified trypsin (Promega) in 5 mM AmBic. The pieces were overlaid with 5 mM AmBic and trypsinised for 16 h at 37°C. Supernatant was collected, peptides further extracted twice with 5% TFA in 50% ACN and supernatants pooled. Peptide extracts were dried, resuspended in 5 μL ddH_2O prior to MS analysis.

2.10 Protein identification by MALDI-MS

MALDI-MS with PMF was used for protein identification. Typically, 0.5 μL of tryptic digest was mixed with 1 μL of matrix solution (saturated aqueous 2,5-dihydroxybenzoic acid) and spotted onto a target plate and dried. Mass spectra were acquired on an Ultraflex TOF/TOF mass spectrometer (Bruker Daltonics) in the reflector mode. The spectrometer was calibrated using calibration mixture 2 from the Sequazyme kit (Applied Biosystems) and internal calibration was carried out using trypsin autolysis peaks at m/z 842.51 and m/z 2211.10. Peaks in the mass range m/z 500–5000 were used to generate a peptide mass fingerprint which was searched against the updated NCBI database using Protein Prospector v3.4.1 MS-Fit (University of California, San Francisco, USA). A positive identification was accepted when $\geq$6 peptide masses matched a particular protein (mass error ±50 ppm, one missed cleavage), matched peptides represented $\geq$25% of the sequence, the sequence was human and the molecular weight matched that of the gel spot.

2.11 Immunoblotting and antibodies

Immunoblotting was used to validate expression differences where antibodies were available. Briefly, extracts separated by 1- or 2-DE were electroblotted onto Immobilon P membrane (Millipore). Membranes were blocked for 1 h with 5% w/v low fat milk in TBS (50 mM Tris pH 8, 150 mM NaCl) plus 0.1% Tween-20 (TBS-T). Membranes were incubated for $\geq$1 h in primary antibody in TBS-T, washed in TBS-T (3 × 10 min) and probed with the appropriate horseradish peroxidase-coupled secondary antibody. After further washes in TBS-T, immunoprobed proteins were visualised using ECL (Perkin-Elmer Life Sciences). Films were scanned on a Bio-Rad GS-800 densitometer and matched to ICy dye images using Adobe Photoshop. Polyclonal antibodies used were anticyclophilin A (Upstate); antiPrxn2 and antiPrxn6 (Prxn – peroxiredoxin) (from Dr. E. Schroder, Wake Forest University School of Medicine, USA); antiPrxn1, 2, 3, 5 and 6 (LabFrontier); antiRan (from Dr. D. Gorlich, University of Heidelberg, Germany, [18]); and antiTPI (from Dr. O. Judit, Institute of Enzymology, Hungarian Academy of Sciences, Hungary). Monoclonal antibodies used were antiprohibitin (Lab Vision); antiHsp70 (Hsp – heat-shock protein) (Sigma); antiHsp27 and antiTCP1-β (both from Stressgen Biotech).

3 Results and discussion

3.1 Development of a cysteine thiol-labelling 2-D DIGE method

Our goal was to develop a fluorescent labelling strategy to improve on the existing 2-D DIGE expression profiling technology. Thus instead of labelling lysine residues at low stoichiometry, our target was to label cysteine thiols at higher stoichiometry without adversely affecting protein solubility or migration behaviour in 2-D gels. We also reasoned that these reagents could be used to probe for inducible changes in the reactivity of protein thiols, allowing us for example, to follow redox modification events such as disulphide bond formation/breakage, glutathionylation or oxidation to the sulphenic (RSOH), sulphinic (RSO_2H) or sulphonic (RSO_3H) acids. Of the two classic thiol-reactive functionalities, we chose to prepare iodoacetyl derivatives of Cy3 and Cy5 for 2-D DIGE (Fig. 1), as opposed to maleimides [7], on the basis of their expected greater reactivity. An outline of the synthesis and the structures of ICy3 and ICy5 and other derivatives are shown in Fig. 1, with a detailed description of the synthesis provided as Supplementary Material. The spectrally distinct ICy dyes are size and charge matched and should have equivalent reactivity for free thiol groups.

We first examined ICy labelling of cell lysates under conditions that could be used for 2-DE analysis. Preliminary 1-D experiments revealed that labelling with ICy3 or ICy5 at 160 pmol/μg protein (a molar ratio of ~10:1 dye to protein for a 60 kDa protein) in nonreducing 2-DE lysis buffer (8 M urea, 4% CHAPS, 10 mM Tris pH 8.3, 1 mM EDTA) reached a steady state within 5–10 min at 0°C (Fig. 2A). Increasing the incubation temperature to 30°C only modestly increased the labelling and so 0°C was used in further studies to limit possible protein carbamylation by the breakdown products of urea in the buffer. A significant number of protein bands were also detected under 'native' labelling conditions (Fig. 2A), suggesting that thiol reactivity could be monitored under more physiological conditions. Of note, thiourea, a denaturant commonly used in 2-DE analysis, totally blocked protein labelling (data not shown). This is likely to result from quenching of the ICy dye by thiourea, as reported for other IAMs [19], but not for the maleimide Cy dyes [7].

3.2 ICy labelling of standard proteins

In order to use the ICy dyes for labelling of proteins, it was crucial to establish an optimal working molar ratio of dye to protein. To establish this, we examined ICy dye labelling of an equimolar mixture of standard proteins containing different numbers of free and disulphide-bridged thiols (BSA, one free thiol/17 disulphides; Ova, four free thiols/1 disulphide; GST, four free thiols; α-Crys A chain, one free thiol; α-Crys B, no thiols; and Myo, no thiols) and compared the extent of labelling with that achieved on lysine residues using NHS-Cy dye. Mixtures of proteins were labelled at increasing dye to protein ratios in a nonreducing, 2-DE lysis buffer. As expected, only the free thiol-containing proteins were labelled to any significant degree, and labelling was equivalent for ICy3 and ICy5 (Fig. 2B and data not shown). However, the fluorescence intensities varied between proteins. For example, GST with four free thiols was detected at higher intensity than Ova, also with four free thiols, whilst BSA with one free thiol was labelled to the greatest extent. Since differential oxidation of the standards may account for this variation, we measured the free thiol content of the proteins using Ellman's reagent (DTNB), which showed that BSA contained 0.61 mol/mol free thiol/protein, Ova 1.67 mol/mol and α-Crys A chain 0.53 mol/mol. Although this indicates partial oxidation, it does not account for the differences in labelling. Whilst we cannot completely rule out nonthiol labelling, our data suggest that free thiol groups display variable reactivity for the dyes, even in 8 M urea. In addition, it appeared that saturation labelling was not attained for any of the targets, even at dye to protein ratios of 1600:1. Maximal lysine labelling was more sensitive than cysteine labelling, but resulted in significant and heterogeneous molecular weight increases to all proteins (at ratios >5:1), presumably as more dye molecules reacted with the higher number of lysines on each protein (Fig. 2B and C). 2-DE gel analysis of the same samples labelled at ratios of 5:1 generated a higher isoform complexity of lysine- *versus* cysteine-labelled proteins. For example, unlabelled and cysteine-labelled α-Crys A chain ran as three isoforms on 2-D gels, whereas at least 12 lysine-labelled isoforms were detected (data not shown).

These results obviously reflect the relative numbers of lysine and cysteine residues in target proteins, but demonstrate the advantage of stoichiometric cysteine labelling, which for most proteins would generate a minimal number of labelled isoforms. Importantly, there was significant protein precipitation at higher dye to protein ratios using both labelling strategies as previously observed for maleimide Cy dye labelling [7]. For this reason, an optimal dye to protein ratio of 5:1 was chosen for further 2-D DIGE optimisation to avoid protein loss and provide a reasonable level of sensitivity. Labelling was also examined after prereduction of disulphide bonds with DTT, which was removed by acetone precipitation of proteins prior to labelling. For these prereduced samples, ICy labelling became more extensive presumably as free thiols were made available (Fig. 2D). These results also indicated that GST and α-Crys A were indeed partially oxidised as previously suggested. However, heterogeneous labelling and variable protein recovery from the precipitation were apparent, and for this reason we chose to pursue only the labelling of free thiol-containing proteins in the absence of reductants.

3.3 Specificity and sensitivity of ICy labelling

The specificity of the ICy dyes was next tested by competition experiments using IAM and DTT. A five-fold molar excess of either reagent led to an almost complete blockade of ICy

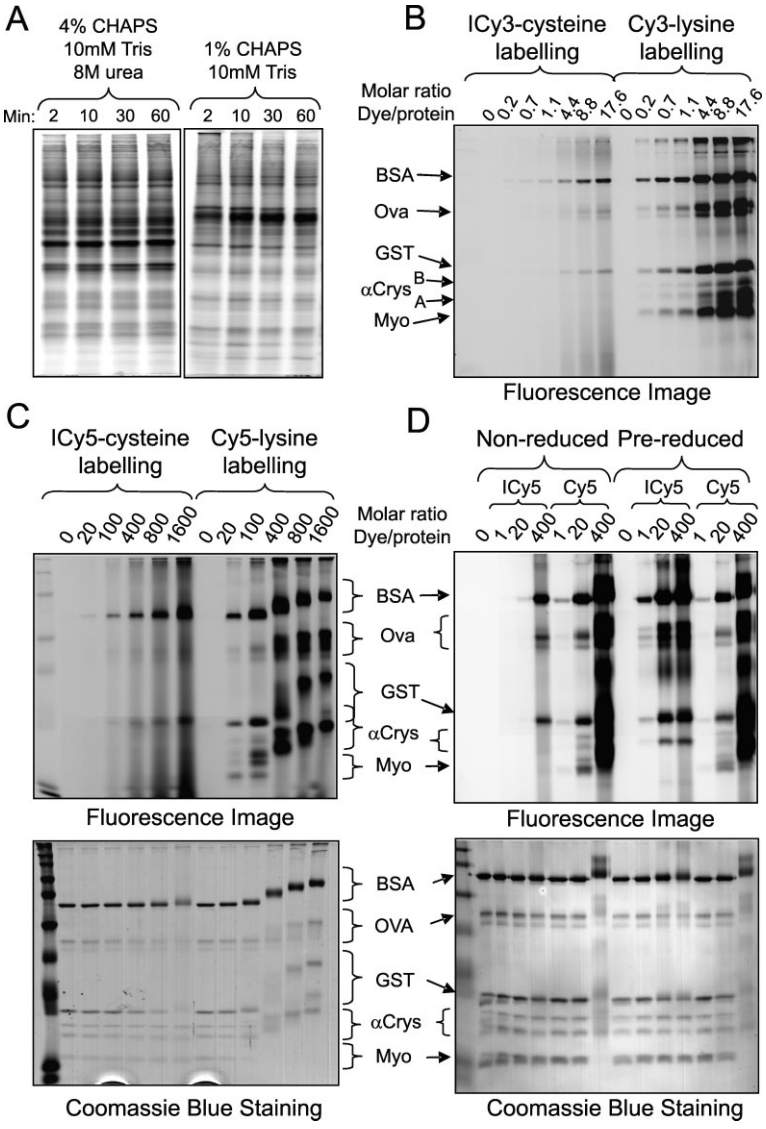

Figure 2. Comparison of cysteine and lysine labellings using ICy and NHS-Cy dyes. (A) Comparison of denatured *versus* native labelling. HB4a cell lysates in 2-D lysis buffer (left panel) or in 1% CHAPS/10 mM Tris pH 8.3 (right panel) were labelled with ICy3 at 160 pmol/μg on ice for the indicated times, and quenched by addition of Laemmli sample buffer. Proteins (10 μg) were resolved by 12% 1-D SDS-PAGE and fluorescent images captured. (B) Labelling of a standard mixture of proteins at increasing molar ratios of ICy3 or NHS-Cy3 dye to protein. An equimolar mixture (0.4 pmol each) of BSA, Ova, GST, α-Crys A/B and Myo in 2-D lysis buffer was labelled at the indicated molar ratios for 1 h on ice. Reactions were quenched with DTT or free lysine and proteins resolved by 12% 1-D SDS-PAGE. Resulting fluorescent image is shown. Although signals were detected in all lanes, a lower intensity image is shown to distinguish bands in the darker lanes. (C) Labelling of the standard mixture was carried out as above, except that higher ratios of ICy5 and NHS-Cy5 were used. A CCB poststained gel is shown. (D) Effect of prereduction on ICy and NHS-Cy dye labelling. Standards were labelled with ICy5 or NHS-Cy5 at the indicated dye to protein ratios without reductant, or after reduction with 65 mM DTT. DTT was removed prior to labelling by acetone precipitation. A CCB poststained gel is shown.

labelling of proteins in unreduced cell lysates, as assessed by 1- and 2-DE (data not shown). We estimated the sensitivity of ICy labelling using BSA and compared this with MS-compatible silver staining and colloidal Coomassie blue G-250 (CCB) staining. Results (Fig. 3A) show that as little as 2 ng of this single free thiol-containing protein was detected with ICy3 or ICy5 using a 5:1 molar excess of dye, a limit that was better than that achieved with silver (~10 ng) or CCB staining (~20 ng). In addition, the dynamic range of detection was identical for the two ICy dyes and broader and more linear compared to silver or CBB staining; these are essential prerequisites for quantifying low- and high-abundant proteins on the same 2-D gel. Although saturation was not reached for BSA labelling, 2-DE DeCyder analysis of lysates showed a dynamic range of 10^3–10^4-fold (data not shown), similar to that reported for the maleimide and NHS-Cy dyes [7].

Comparison of 2-D ICy images of cell lysates with the composite silver-stained images showed that a significant number of protein spots were detected at a higher sensitivity with ICy labelling than silver staining (arrows in Fig. 3B). To explore this phenomenon further and to test the labelling properties of the ICy dyes for 2-D DIGE application, we carried out a detailed 2-DE analysis comparing ICy dye labelling with NHS-Cy labelling, and with silver, CCB and SYPRO Ruby poststaining. This analysis (Fig. 3C) revealed that similar numbers of cysteine-labelled, lysine-labelled and CCB-stained features could be detected (903–1034 spots); with silver staining performing slightly better (1205 ± 78). However, only ~50% of ICy-labelled features comigrated with spots detected using the other methods. This difference is attributable to detection of nonfree thiol-containing proteins using the other methods and proteins that stain poorly with silver. However, since the total number of detected spots was

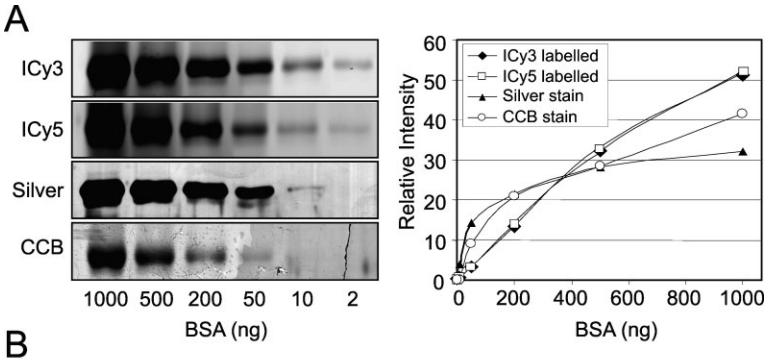

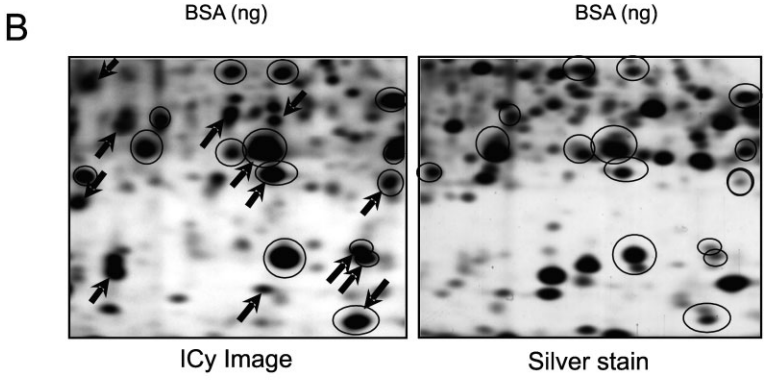

C

Comparison of ICy, NHS-Cy, silver and CCB labelling/staining

	No. of detected spots (Silver, NHS-Cy or CCB)	No. of ICy-labelled spots on same gel	No. of co-migrating spots	% Match
Silver	1205±78	1034±245	470±56	45.5%
NHS-Cy dye	956	980	551	56.2%
CCB	900	903	414	45.8%

Figure 3. Characterisation of ICy dye labelling. (A) Sensitivity test of ICy dyes. BSA was labelled at a 5:1 molar ratio of ICy3 and ICy5, and the indicated amounts of labelled BSA resolved on a 1-D gel. Gels were poststained with either CCB or silver (left panel) and relative band intensities from fluorescent images or densitometry were plotted against protein amounts (right panel). (B) Comparison of comigrating spot intensities. HB4a cell lysate (200 μg) was labelled with 16 nmol of ICy3 (80 pmol/μg) and separated by 2-DE and the gel poststained with silver for comparison of spot migration. 'Landmark' features are circled and arrows indicate features detected with higher intensity by ICy labelling. (C) Comparative 2-DE analysis of ICy and NHS-Cy labelling, silver and CCB staining. HB4a cell lysates (200 μg) were labelled with ICy3 and NHS-Cy5 at ratios of 80 and 4 pmol/μg respectively, and separated on the same 2-D gel. Replicate ICy-labelled samples were also resolved and poststained with silver or CCB. Images were analysed with Melanie IV software and spots matched to the corresponding NHS-Cy-labelled, silver-stained or CCB-stained spots on each gel. Total numbers of spots were taken for each detection method, and the number of comigrating spots and the% match calculated. ICy3-silver stain pair was repeated three times with average spot numbers ± SD shown.

similar, it is likely that a significant subset of proteins with reactive thiols can only be detected by ICy labelling, as implied from Fig. 3B. However, there is a further level of complexity in that the ICy dyes are positively charged such that labelled proteins may shift to more basic p*I*s. Assuming substoichiometric ICy labelling, this would cause dilution and loss of detection of the comigrating silver-stained spots, whilst leaving an unlabelled pool of silver-stainable protein. SYPRO Ruby poststaining yielded poor images where intense ICy-labelled features appeared as 'inverse spots' (data not shown); this effect may result from fluorescence quenching of the SYPRO Ruby signal.

3.4 Differential labelling with ICy3 and ICy5

Having established conditions for 2-DE labelling, we next assessed how the ICy dyes would perform in 2-D DIGE experiments. Initially, we compared ICy3-labelled lysates of HB4a (an immortalised HMLEC line) with ICy5-labelled lysates of C3.6 (an ErbB2 overexpressing derivative of HB4a) (Fig. 4A). Many high-intensity ICy-labelled protein features were detected (700–800 spots) indicating that a significant number of cellular proteins and isoforms possess reduced, reactive thiols in exponentially growing epithelial cells. The overall signal intensity was higher than for minimal lysine labelling, although basic charge trains were apparent for some higher molecular weight proteins (Fig. 4A). Since the ICy dyes are positively charged, these basic shifts may reflect partial labelling of proteins with multiple reactive thiols. Clear differences in the expression of some proteins were apparent between the cell lines indicative of ErbB2-dependent expression changes (see below). To test for differences in the reactivities of ICy3 and ICy5, lysate from the same cells (HB4a) was labelled with ICy3 and ICy5 and the mixed samples separated by 2-DE. Image comparison using DeCyder software (Fig. 4B) suggested that a small subset of the same protein species (8% over a 1.5-fold threshold; 1% over a two-fold threshold) was preferentially labelled by one dye over the other. This suggests that ICy3 and ICy5 can display different reactivities against some proteins, as previously reported for the maleimide Cy dyes [7]. It is possible that intermolecular fluorescence resonance energy transfer between Cy3 and Cy5 or fluorescence quenching of Cy fluorophores on the same multiply-labelled molecule may account for this. However,

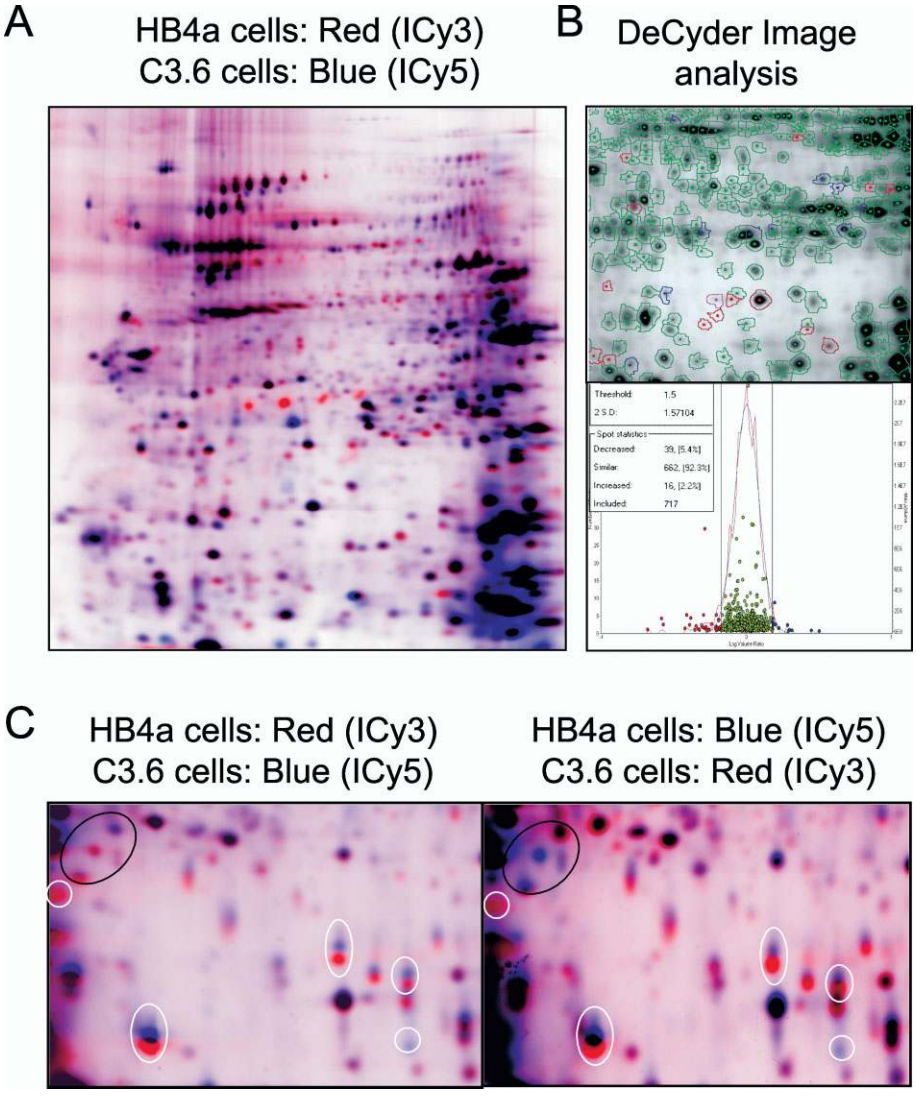

Figure 4. Differential ICy3 and ICy5 labellings. (A) 2-D DIGE analysis of HB4a and C3.6 cell lines. HB4a and C3.6 cell lysates were labelled with ICy3 and ICy5, respectively, and the samples mixed and resolved by 2-DE. Images were captured at the appropriate excitation and emission wavelengths and pseudocoloured (HB4a in red; C3.6 in blue) and overlaid in Adobe Photoshop. (B) Analysis of preferential ICy dye labelling. Identical lysates labelled with ICy3 and ICy5 were mixed and resolved by 2-DE and analysed using DeCyder DIA software. Differences were examined using a 1.5-fold and two-fold cutoff. A section of the image and spot statistics are shown. Green denotes no significant difference between comigrating spots, while blue and red denote increased and decreased intensity respectively. (C) Dye bias and spot splitting revealed by reciprocal labelling. HB4a and C3.6 lysates were reciprocally labelled with ICy3 and ICy5, mixed appropriately and resolved by 2-DE. Images were captured, pseudocoloured and overlaid in Adobe Photoshop for comparison. Black-circled spots represent real differences and white-circled spots indicate dye bias and spot splitting.

overlaying the images of reciprocally-labelled HB4a or C3.6 lysates revealed that much of this apparent dye bias resulted from separation of ICy3- and ICy5-labelled proteins into doublets (specifically in the 25–30 kDa range) with the ICy3-labelled pool migrating faster (Fig. 4C). One hypothesis for this could be that SDS could interact differently with the two differentially labelled protein pools and affect their migration in gels. This effect was reproducible in that the same protein features displayed preferential labelling/spot splitting in multiple analyses. It is however important to note that our 2-D DIGE experiments are designed to remove these 'false' differences, since test samples for comparison are labelled with the same ICy dye and run against a standard pool labelled with the other dye, as used previously with the NHS-Cy dyes [3, 6].

Comparison of our labelling strategy with that used for the recently reported maleimide Cy dyes [7] revealed similar findings, including increased sensitivity of detection of thiol-containing proteins, increased protein precipitation at high labelling ratios, altered 2-DE spot patterns compared with minimal lysine labelling and some apparent dye bias. A major difference between this and our approach is that the maleimide dyes have been used for labelling of all cysteine-containing proteins in prereduced samples, whereas our focus was on the labelling of nonreduced samples with a view to following redox-dependent thiol reactivity. This is likely to affect the reactivity and extent of labelling. As such, we opted to use a lower dye to protein ratio and did not see the appreciable sample losses due to precipitation as reported by Shaw *et al.* [7]. It is also worth noting that the maleimide dyes are sulphonated to give them a net neutral charge, and so they have the advantage that they should not alter the p*I* of labelled proteins, unlike the ICy dyes, where potential p*I* shifts will add complexity to our analysis. We have yet to explore labelling of fully reduced lysate samples using our reagents, or to compare the two reagent sets directly.

3.5 Application of cysteine-labelling 2-D DIGE

We next applied the optimised ICy-labelling protocol in a detailed 2-D DIGE and MALDI-TOF MS analysis to accurately and simultaneously identify changes in thiol reactivity and protein expression in response to H_2O_2 treatment and ErbB2 overexpression in mammary luminal epithelial cells. These studies were aimed at identifying cellular targets of oxidative stress and the protective mechanisms that respond to redox insult, and to simultaneously screen for targets of ErbB2-mediated growth factor signalling and assess its possible impact on the redox response. In a preliminary time-course experiment, HB4a and C3.6 cells were treated with 0.5 mM H_2O_2 for 2, 20 and 240 min or left untreated. These conditions were sufficient to induce an increase in total cellular tyrosine phosphorylation (likely through inhibition of protein tyrosine phosphatases), and trigger activation of the p38 stress-activated protein kinase, ERK1/2 and Akt signalling pathways (data not shown). Notably, HB4a cells displayed more rapid and higher levels of ERK1/2 and p38 activation, suggesting that ErbB2 can modulate stress-activated signalling. Duplicate cultures of treated cells were lysed under nonreducing, denaturing conditions in the presence of ICy3 and ICy5 (80 pmol/μg protein) to rapidly label proteins and limit postlysis redox modification. Samples were then reduced with DTT for 2-DE separation. Individual ICy5-labelled samples were run with an equal load of ICy3-labelled standard pool consisting of an equal mixture of all samples. Image analysis revealed over 100 differences (≥1.5-fold) both between cell lines (ErbB2-dependent) and with H_2O_2 treatment. A pseudocoloured and overlaid area of the images for the C3.6 samples is shown for each time-point in Fig. 5A. Of particular note, H_2O_2 treatment for only 2 min reduced the labelling of a number of proteins suggestive of rapid oxidation-dependent thiol modifications that block ICy-labelling, rather than changes in protein expression *per se*. Such modifications would include disulphide bond formation, modification by glutathionylation or oxidation to the sulphenic (R-SOH) acid; the latter modification is generally unstable and may form a disulphide with a nearby thiol or is further oxidised to the sulphinic ($R\text{-}SO_2H$) or sulphonic ($R\text{-}SO_3H$) acid. In some cases, the change in ICy labelling recovered over time, indicating reversible modification. Interestingly, a number of proteins showed a rapid increase in labelling (Fig. 5A), suggesting generation of new thiols, for example *via* scission of disulphides or through labelling of isoforms generated by redox-dependent shifts in p*I*, as reported for the Prxns [20, 21].

Experiments were repeated at the 0 and 20 min time-points in triplicate using both cell lines (12 samples) to simultaneously examine significant changes due to ErbB2 overexpression and H_2O_2 treatment, and for excision of protein spots for MS identification. Three independent experiments were run with very similar changes observed in all three. In one experiment, 126 significant changes in labelling were identified (>1.5-fold up- or down-regulated; $p < 0.05$). Of these, 56 were peroxide-dependent and 94 ErbB2-dependent, with 24 changes displaying dual dependency. Poststaining with silver or CCB and matching to the corresponding fluorescent images allowed picking of 89 gel features with confidence, and we identified 51 proteins by MALDI-TOF peptide mass mapping (see Section 2), representing 38 individual gene products. Around half of the proteins displaying differential labelling were identified in more than one experiment, confirming the reproducibility of the labelling strategy. Proteins that could not be identified were generally of low abundance (as determined by poststaining) and gave low ion intensities by MS. Thus, detection of changes in low-abundance thiol-containing proteins was possible, although the processing steps and MALDI-TOF analysis were insufficiently sensitive to identify them. We propose that affinity methods could be employed to enrich such species, and indeed, our preliminary experiments with cleavable, biotinylated versions of the ICy dyes suggest that this may be possible (data not shown).

3.6 Peroxide-dependent changes in thiol reactivity and protein expression

Combined results of MALDI-MS analysis for the three independent experiments are shown in Table 1A and B, for H_2O_2- and ErbB2-dependent changes, respectively. Examples of these changes are presented graphically in Fig. 5B, whilst Fig. 5C shows the 2-DE migration of all identified proteins. It is important to note that all proteins identified contain at least one free cysteine thiol, validating the labelling specificity. Proteins differentially labelled or expressed in response to H_2O_2 fell into several functional groups. Firstly, the molecular chaperones: Hsp73/71, ER chaperone BiP/Grp78, peptidyl-prolyl *cis-trans* isomerase A (cyclophilin A – CypA), signal recognition particle receptor β subunit (SRβ) and the T-complex protein 1 (TCP1) subunits α, β, γ and ζ involved processes such as ATP-dependent protein folding, protein transport, degradation of incorrectly folded polypeptides and prevention of aggregation of newly synthesised polypeptides. ICy labelling was both increased and reduced by H_2O_2 treatment depending on the particular protein (Table 1A and Fig. 5B). CypA showed the greatest increase in labelling in response to H_2O_2 and immunoblotting revealed that this was not due to altered protein expression, although differential labelling between cell lines did appear to result from a change in protein expression (Fig. 6A). The increased labelling is difficult to explain given that CypA contains only free thiols, and suggests a more complex mechanism of redox modulation. One possibility is that H_2O_2 may cleave a disulphide bond between CypA and another protein or release a mixed disulphide such as GSH, to liberate a free thiol. In support of this, CypA can bind to and promote the antioxidant activity of Prxns [22]. The modulation of molecular chaperones by H_2O_2 is likely to affect protein folding and may trigger the unfolded protein response (UPR) that modulates expression of ER chaperones such as BiP/Grp78 and

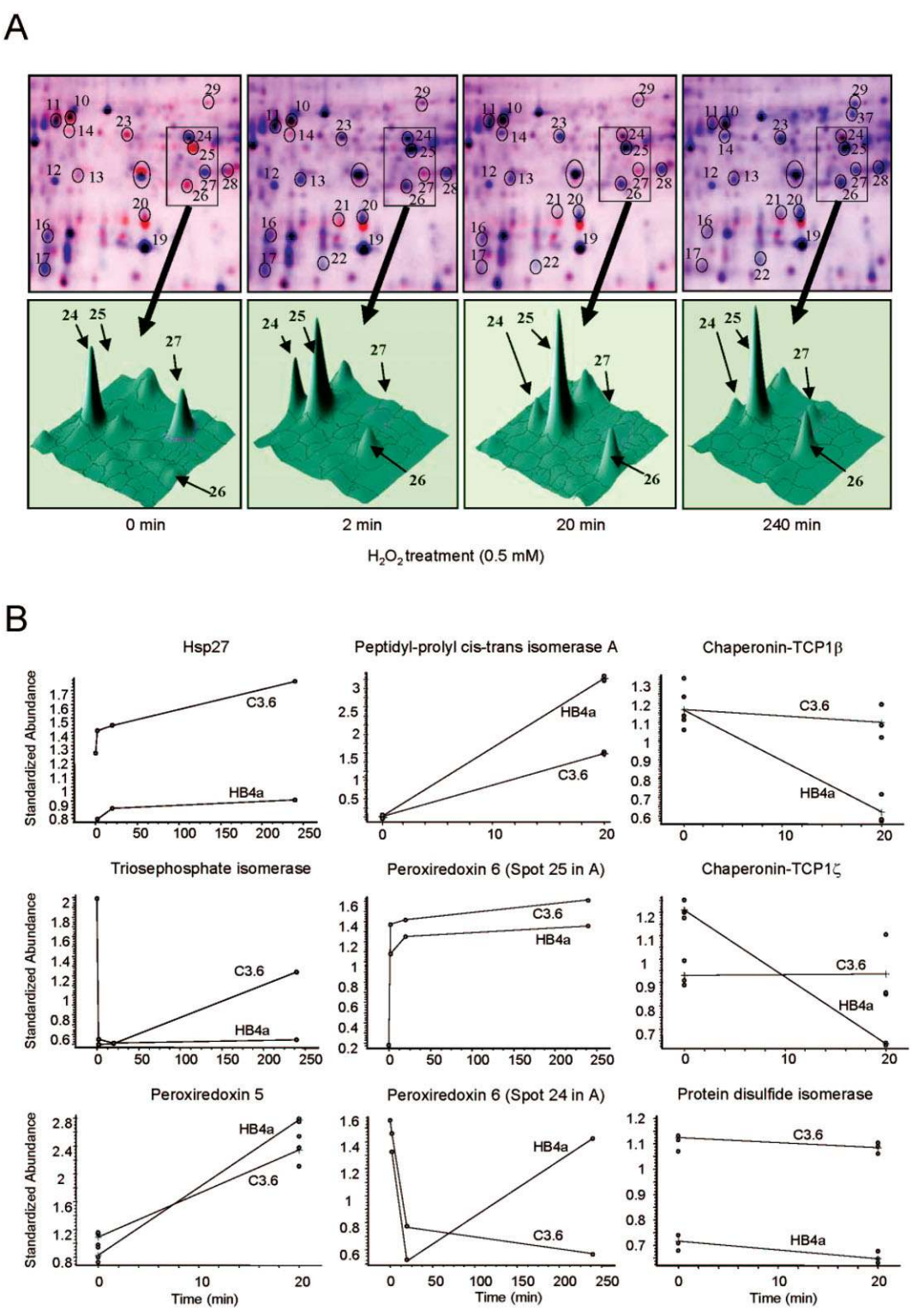

Figure 5. Multiplex 2-D DIGE analysis to monitor oxidant-dependent thiol reactivity and ErbB2-dependent expression in HMLECs. (A) Sections of pseudocoloured and overlaid 2-D DIGE images and 3-D fluorescence profiles of C3.6 cell lysates from untreated cells (0 min) and cells treated with 0.5 mM H_2O_2 for 2, 20 and 240 min are shown. Individual lysates were labelled with ICy5 (blue) and compared with a standard pool on each gel labelled with ICy3 (red). (B) Examples of proteins displaying altered labelling following H_2O_2 treatment and/or differential expression between HB4a and C3.6 cell lines. Proteins were identified from gels by MALDI-MS as described

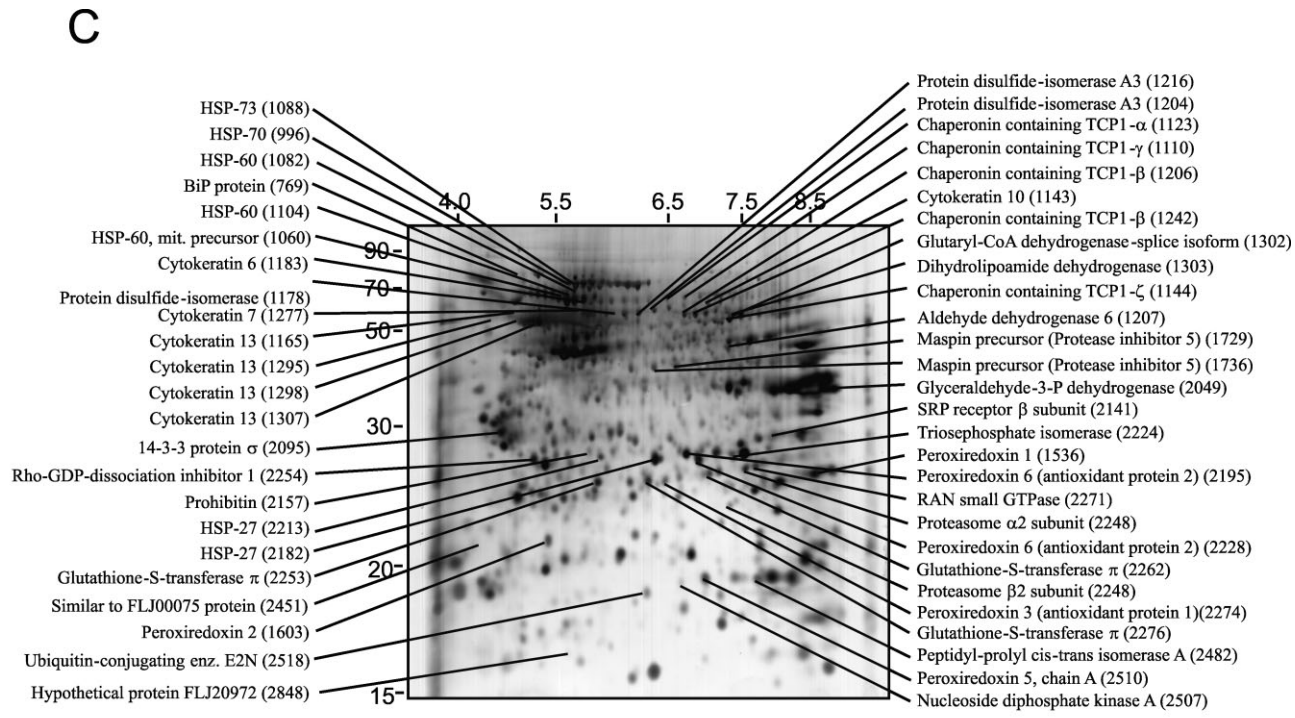

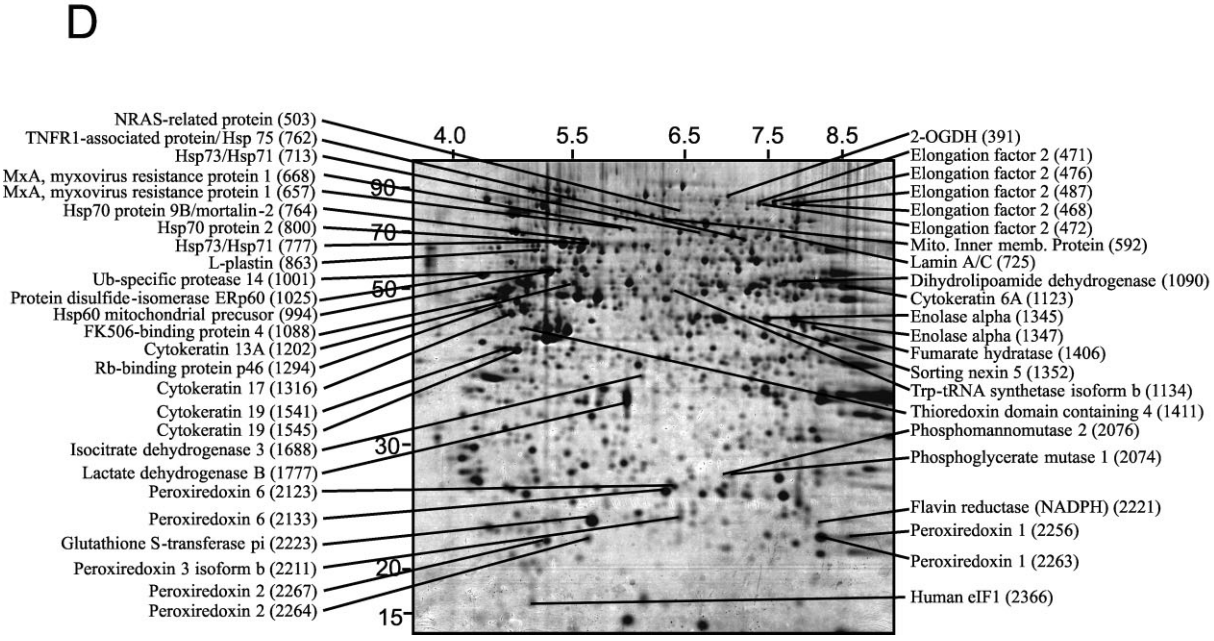

in Section 2. Graphs were derived from DeCyder analysis where the standardised abundance is the ratio of the volume of test *versus* standard gel features. Triplicate data points are shown for the 0 and 20 min experiments with lines joining average values, whilst single data points are shown from a preliminary time-course experiment. (C) 2-DE migration of proteins identified by ICy 2-D DIGE and MS displaying H_2O_2-induced differential labelling and ErbB2-dependent expression (see Table 1). A representative silver-stained gel is shown. (D) 2-DE migration of proteins identified by NHS-Cy 2-D DIGE and MS (see Table 2). A representative CCB-stained gel is shown.

the protein disulphide isomerase PDI/ERp60 (see below) allowing cells to tolerate accumulation of unfolded proteins [23]. It is of interest that BiP/GRP78 has been shown to play an important role in the UPR by providing cytoprotection from H_2O_2 in a mechanism involving activation of ERK1/2 signalling [24].

Importantly, a number of the identified proteins have known roles as cellular redox regulators, including two isoforms of GST π, where labelling was reduced after H_2O_2 treatment and which were down-regulated in the C3.6 cells, and five of the six known Prxn family members. The Prxns are antioxidant enzymes that function by reducing hydroperoxides and have been implicated in redox-regulation of cell signalling [25]. ICy dye labelling of 2-DE isoforms corresponding to Prxn1, 2, 3, 5 and 6 was increased after H_2O_2 treatment, whilst another isoform of Prxn6 was reduced (Table 1A and Fig. 5B). 1-D immunoblotting showed that overall Prxn expression did not correlate with ICy labelling; Prxn1 and 3 levels were slightly increased by H_2O_2 treatment, whilst that of Prxn2 was decreased and Prxn5 and 6 were unaffected (Fig. 6B). All Prxns contain an active-site cysteine which is oxidised to a sulphenic acid by the peroxide substrate which is regenerated back to the free thiol *via* various mechanisms, including intramolecular and intermolecular disulphide bond formation and reduction by the thioredoxin system. Previous data have shown that Prxn cysteines can be overoxidised to sulphinic or sulphonic acids, resulting in an acidic shift on 2-D gels [20, 21]. Whilst it is expected that H_2O_2-dependent oxidation of Prxn active-site cysteines would block ICy labelling, we hypothesise that the increased labelling observed may occur as a result of labelling of other free thiols (present in all Prxns) on a p*I*-shifted pool of oxidised protein.

Other proteins of interest modified by peroxide treatment included glyceraldehyde 3-phosphate dehydrogenase (G3PDH), triosephosphate isomerase (TPI), prohibitin, and Ran, which displayed the greatest H_2O_2-dependent decrease in ICy labelling. TPI, Ran and prohibitin expression were found not to be altered significantly by H_2O_2 treatment, suggestive of direct oxidative modification (Fig. 6B). In support of this, we observed reduced ICy labelling of recombinant Ran protein after treatment with H_2O_2 (data not shown). The modulation of the glycolytic enzymes G3PDH and TPI supports previous data showing that oxidative stress can redirect carbohydrate fluxes to generate increased reducing power in the form of NADPH at the expense of glycolysis [26, 27]. Prohibitin is a repressor of E2F-mediated transcription and is implicated in cell cycle regulation, senescence, immortalisation and tumourigenesis (reviewed in [28]). Its oxidative modification may therefore have profound effects on cellular proliferation. Likewise, the small GTPase Ran plays a critical role in active nuclear transport [18, 29], and its modification may adversely affect protein localisation or be part of a redox protective mechanism. SRβ is also a small GTPase involved in targeting of nascent polypeptides to the ER translocation machinery [30]; we propose therefore that GTPases may be novel targets of oxidative stress and the impact of redox modification of these enzymes on protein localisation and processing merits further analysis.

3.7 ErbB2-dependent changes in thiol reactivity and protein expression

Our experimental strategy allowed simultaneous comparison of the effects of ErbB2 overexpression on the proteome of cells exposed to oxidative stress. We identified 26 gene products (representing 36 isoforms) that were up- or down-regulated (>1.5-fold; $p < 0.05$) in untreated or H_2O_2-treated normal (HB4a) *versus* ErbB2 overexpressing (C3.6) cells (Table 1). As with H_2O_2, there was differential modulation of several molecular chaperones, suggesting that ErbB2 overexpression may alter protein folding/processing and influence the stress response. For example, multiple isoforms of Hsp27 (possibly due to phosphorylation) and PDI/ERp60 were up-regulated in the C3.6 cells and moderately affected (1.2–1.5-fold) by H_2O_2; Hsp60 and Hsp73/71 were down-regulated and unaffected by H_2O_2; and TCP1-α, TCP1-β, SRβ and CypA showed both robust ErbB2- and H_2O_2-dependent regulations (Table 1 and Fig. 6). Although the functional consequences of these changes are unclear, several of these stress-response proteins have been shown to be dysregulated in human cancer and appear to alter the response of tumour cells to immune surveillance, anticancer drugs and oxidative stress (reviewed in [31]). Indeed, Hsp27 is overexpressed in invasive ductal carcinomas of the breast [31] and protects cells against oxidative stress through p38-dependent phosphorylation and cytoskeletal modulation [32, 33].

Isoforms of several redox regulatory proteins (GSTπ, Prxn3, Prxn6, Rho-GDP-dissociation inhibitor 1 (RhoGDI1) and dihydrolipoamide dehydrogenase) were also altered by ErbB2 overexpression, although 1-D immunoblotting of total protein expression did not always agree with ICy labelling data (*e.g.* the Prxns in Fig. 6B), presumably because differentially labelled isoforms cannot be resolved by 1-DE or labelling is altered by thiol modification rather than changes in protein abundance. Dysregulated expression of Prxns has been observed in human cancers, including breast cancer, and has been correlated with a protective role against antitumour agents and oxidants, and was even reported to promote cell proliferation and tumour progression [34–36]. Whilst changes in Prxn expression and redox signalling may be responsible for the hyperproliferative phenotype observed in the C3.6 cells [37], down-regulation of 14-3-3σ, a negative regulator of cell proliferation (Table 1B), could also play an important role. Indeed, and in agreement with our findings, 14-3-3σ expression was down-regulated in a significant proportion of primary breast carcinomas [38, 39], and it is tempting to speculate that ErbB2 overexpression may directly cause this down-regulation.

Table 1. Differentially labelled/expressed proteins identified by ICy 2-D DIGE and MS. (A) Proteins displaying H_2O_2-induced differential labelling in normal (HB4a) and ErbB2-overexpressing (C3.6) HMLECs. (B) Proteins displaying differential labelling between HB4a and C3.6 luminal epithelial cells. Proteins were identified by MALDI-TOF peptide mass mapping (see Section 2)

A

Spot no	Protein name	% Cov	Est. mass	Est. p*I*	Pred. Mass	Pred. p*I*	GI No.	Average fold-difference[b] 4a(20′) to 4a(0)	3.6(20′) to 3.6(0)	3.6(0′) to 4a(0)	3.6(20′) to 4a(20′)	Function
769	BiP/Grp78[a]	35	72000	5.1	70932	5.2	6470150	1.49	1.71	-1.08	1.06	Protein folding
1123	Chaperonin containing TCP1-α	33	60000	6.7	60344	5.8	135538	-1.6	-1.09	1.12	1.65	Protein folding
1242	Chaperonin containing TCP1-β [a]	50	55000	6.8	57489	6	5453603	-1.88	-1.06	1	1.77	Protein folding
1206	Chaperonin containing TCP1-β [a]	50	55000	6.7	57489	6	5453603	N.A.	1.55	N.A.	1.55	Protein folding
1110	Chaperonin containing TCP1-γ	25	57000	6.6	60403	6.1	20455521	-1.5	-1.1	1.09	1.48	Protein folding
1144	Chaperonin containing TCP1-ζ	43	56000	7.2	58025	6.2	730922	-1.91	1.01	-1.31	1.47	Protein folding
1143	Cytokeratin 10	28	58000	6.9	58827	5.1	4557697	-1.74	-1.34	1.1	1.43	Cytoskeleton
2276	Glutathione S-transferase π	55	25000	6.4	24678	5.7	121746	-1.61	-1.27	-1.78	-1.4	Regulation of cellular redox state
2253	Glutathione S-transferase π	54	25000	5.7	23225	5.4	121746	-1.55	-1.45	-1.7	-1.59	Regulation of cellular redox state
2049	Glyceraldehyde-3-phosphate DH[a]	42	35000	9	36054	8.6	120649	1.53	N.A.	N.A.	N.A.	Glycolysis
1088	Hsp73/Hsp71[a]	46	70000	6	70898	5.4	123648	-1.84	N.A.	N.A.	N.A.	Protein folding
2482	Peptidyl-prolyl cis-trans isomerase A[a]	65	15000	8	17881	7.8	13937981	16.19	7.36	1.09	-2.01	Protein folding/conformation
1536	Peroxiredoxin 1[a]	42	23000	8.6	22111	8.3	548453	4.82	N.A.	N.A.	N.A.	Protection from oxidative stress
1603	Peroxiredoxin 2[a]	48	20000	6	21892	5.7	2507169	14.67	N.A.	N.A.	N.A.	Protection from oxidative stress
2274	Peroxiredoxin 3 (antioxidant protein 1)	33	26000	6.4	27693	7.7	2507171	2.76	7.37	-2.13	1.25	Protection from oxidative stress
2510	Peroxiredoxin 5[a]	44	17000	7.2	16900	7	15826629	3.42	2.15	1.32	-1.21	Protection from oxidative stress
2195	Peroxiredoxin 6 (antioxidant protein 2)	68	26000	6.9	25035	6	1718024	-2.74	-2.19	1.35	1.69	Protection from oxidative stress
2228	Peroxiredoxin 6 (antioxidant protein 2)	27	27000	7	25035	6	1718024	3.69	4.58	-1.43	-1.15	Protection from oxidative stress
2157	Prohibitin	44	30000	5.6	29804	5.6	4505773	2.69	2.95	-1.1	1	Suppression of proliferation
1563	Proteasome β 2 subunit[a]	49	22000	7.5	22836	6.5	1709762	-2.27	N.A.	N.A.	N.A.	ATP/ubiquitin-dep. proteolysis
2271	Ran small GTPase	57	25000	7.6	24423	7	5453555	-5.55	-3.97	-1.3	1.07	Nucleo-cytoplasmic transport
2141	Signal recognition particle receptorβ subunit	33	29000	8.1	29651	9.2	20141812	2.88	1.68	-1.05	-1.81	SRP-association with membrane
2451	Similar to FLJ00075 protein	38	18000	4.1	17356	4.7	27477376	2.18	1.09	1.34	-1.49	Unknown
1302	Splice isoform of Glutaryl-Co A DH	36	50000	7.3	47356	8.6	2492631	-1.54	-1.35	-6.43	-5.63	Oxidative metabolism
2224	Triosephosphate isomerase[a]	51	28000	7.4	26539	6.5	136060	-2.85	-3.68	1.37	1.06	Glycolysis

B

Spot no.	Protein name	% Cov	Est. mass	Est. p*I*	Pred. Mass	Pred. p*I*	GI No.	Average fold-difference[b] 4a(20′) to 4a(0)	3.6(20′) to 3.6(0)	3.6(0′) to 4a(0)	3.6(20′) to 4a(20′)	Function
2095	14-3-3 σ	31	30000	4.6	27774	4.7	5454052	1.01	-1.15	-1.71	-2	Suppression of proliferation
1207	Aldehyde dehydrogenase 6	25	54000	7.4	56010	6.6	4502041	-1.41	-1.12	1.43	1.81	Aldehyde detoxification
1183	Cytokeratin 6	53	55000	6.1	53501	5.4	14318422	1.04	1.11	1.6	1.72	Cytoskeleton
1277	Cytokeratin 7[a]	54	55000	6.1	51335	5.4	20178293	-1.25	-1.16	1.45	1.57	Cytoskeleton
1307	Cytokeratin 13	34	50000	4.9	49587	4.9	24234696	-1.05	-1.13	4.15	3.87	Cytoskeleton
1298	Cytokeratin 13	30	50000	4.8	49587	4.9	24234696	-1.01	-1.11	3.17	2.88	Cytoskeleton
1295	Cytokeratin 13	31	50000	4.9	49587	4.9	24234696	1.3	-1.06	5.54	4.03	Cytoskeleton
1165	Cytokeratin 13	30	55000	4.9	49587	4.9	24234696	1.05	1.04	2.29	2.28	Cytoskeleton
1303	Dihydrolipoamide dehydrogenase	30	54000	7.5	54151	7.6	118674	-1.04	1.18	-1.84	-1.51	Regulation of cellular redox state
2262	Glutathione *S*-transferase π	36	26000	7.2	24678	5.7	121746	-1.47	-1.12	-2.36	-1.8	Regulation of cellular redox state
2182	Hsp27[a]	46	27000	6.6	22783	6	4504517	-1.31	-1.46	2.51	2.25	Protein folding
2213	Hsp27[a]	24	27000	6.1	22783	6	4504517	1.37	-1.12	6.42	4.2	Protein folding
1104	Hsp60, mitochondrial precursor	22	60000	5.4	61055	5.7	129379	-1.26	-1.05	-1.89	-1.58	Protein folding
1060	Hsp60, mitochondrial precursor[a]	42	57000	5.7	61213	5.7	129379	1.11	-1.07	-1.53	-1.82	Protein folding
1082	Hsp60, mitochondrial precursor[a]	40	57000	5.4	61213	5.7	129379	-1.03	-1.04	-1.77	-1.78	Protein folding
996	Hsp73/Hsp71[a]	44	71000	5.4	70899	5.4	5729877	1.1	-1.13	-1.44	-1.79	Protein folding
2848	Hypothetical protein FLJ20972	35	16000	5.2	16030	5.3	13376554	1.03	-1.01	1.67	1.61	Unknown
1736	Maspin precursor (protease inhibitor 5)	30	41000	6.6	42229	5.8	453368	-1.28	1.08	1.48	2.04	Suppression of proliferation
1729	Maspin precursor (protease inhibitor 5)	63	41000	6.7	42229	5.8	547892	-1.07	1.09	1.4	1.64	Suppression of proliferation
2507	Nucleoside diphosphate kinase A	32	16000	6.6	17149	5.8	127981	1.27	-1.05	1.89	1.42	Nucleotide metabolism
2248	Proteasome α2 subunit	32	26000	7.4	25899	6.9	4506181	1.13	1.07	-2	-2.12	ATP/ubiquitin-dep. proteolysis
1204	Protein disulfide-isomerase ERp60[a]	37	55000	6.5	56783	6	2507461	-1.28	-1.23	1.57	1.64	Disulfide bond formation/protein folding
1216	Protein disulfide-isomerase ERp60[a]	46	56000	6.3	56783	6	2507461	-1.09	-1.02	1.56	1.66	Disulfide bond formation/protein folding
1178	Protein disulfide-isomerase ERp60	25	56000	6.2	56680	6.1	2507461	1.12	-1.04	1.57	1.34	Disulfide bond formation/protein folding
2254	Rho-GDP-dissociation inhibitor 1	31	27000	5	23207	5	4757768	1.33	-1.07	2.01	1.41	NADPH oxidase/small GTPase inhibition
2518	Ubiquitin-conjugating enzyme E2N	55	16000	6.4	17138	6.1	2501432	1.01	1.13	1.74	1.94	Ubiquitin conjugation

a) Proteins identified in two or more independent experiments. Proteins appearing more than once were identified as isoforms with different p*I*s % Coverage of analysed peptides, the estimated mass and p*I* (from gels), the predicted mass and p*I* (from database) and the gene identifier (GI) are shown for each protein.

b) Average fold-differences of replicate samples run on different gels from DeCyder analysis show abundance ratios for treated HB4a cells *versus* untreated (4a(20′)–4a(0)), treated C3.6 cells *versus* untreated (3.6(20′)–3.6(0)), untreated C3.6 *versus* untreated HB4a (3.6(0)–4a(0)) and treated C3.6 *versus* treated HB4a (3.6(20′)–4a(20′)). Proteins displaying an average fold-difference of $\geq$1.5-fold up (+) or down (−) regulation where $p < 0.05$ and spots matched in all images are shaded grey. N.A., not analysed. Functions were ascribed from the NCBInr and Swiss-Prot databases and literature searches.

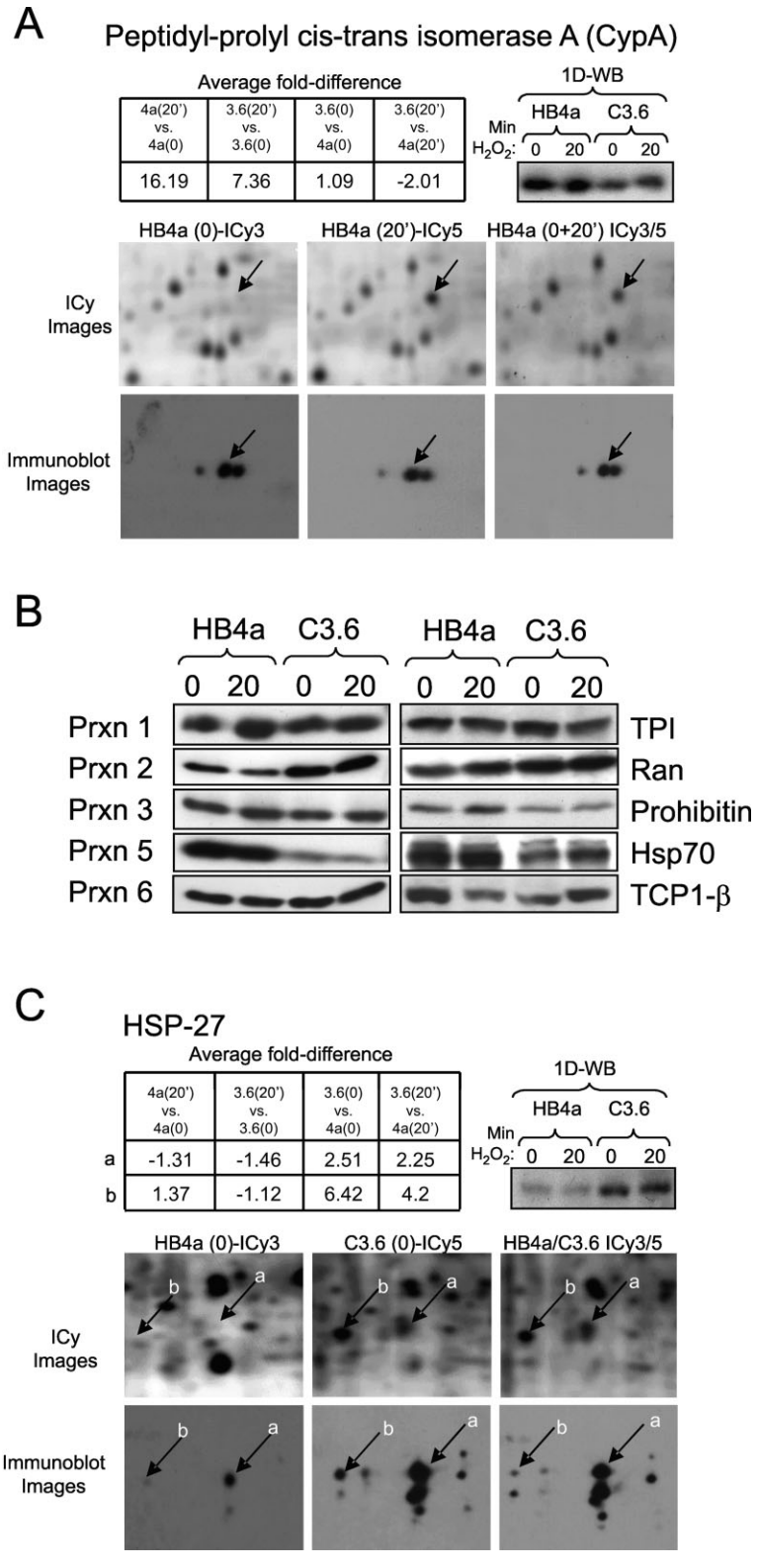

Figure 6. Validation of differential labelling/expression. (A) Peptidyl-prolyl *cis-trans* isomerase A (CypA) expression analysed by 1- and 2-D immunoblotting. 2-D blots of lysates from untreated and H_2O_2-treated HB4a cells and mixed lysate are shown aligned with ICy dye images. Average fold-differences are taken from Table 1A (B) Prxn1, 2, 3, 5 and 6, TPI, Ran, prohibitin, Hsp70 and TCP1-β expression analysed by 1-D immunoblotting of lysates from untreated and H_2O_2-treated HB4a and C3.6 cells. (C) Hsp27 expression analysed by 1- and 2-D immunoblotting. 2-D blots of lysates from untreated HB4a and C3.6 cells and a mixed lysate are shown aligned with the corresponding ICy dye fluorescence images. Average fold-differences are taken from Table 1B.

3.8 Identification of ICy dye-modified cysteine residues

In an attempt to identify the specific sites of redox modification, all MS database searches were conducted with the inclusion of the ICy3/5 modification. However, searches revealed only two potentially modified peptides at low confidence and unlabelled forms of the peptides were also present (data not shown). We suspect that the poor recovery may be due to the lowered solubility and inefficient extraction of labelled peptides from gel pieces, since model peptides labelled in solution performed well in MALDI-TOF experiments (data not shown). Moreover, we did not detect labelling of noncysteine-containing model peptides under the same conditions, supporting the specificity of these reagents for thiol groups. Future refinements to the extraction procedure may improve the yield of labelled peptides, whilst application of MS/MS sequencing would be required to identify sites with higher confidence.

3.9 Analysis of peroxide and ErbB2-dependent changes using NHS-Cy 2-D DIGE

In order to assess the protein labelling changes identified by ICy dye 2-D DIGE and to potentially identify additional H_2O_2- and ErbB2-dependent changes, we also carried out an NHS-Cy dye 2-D DIGE analysis. Fresh HB4a and C3.6 lysates were prepared in triplicate from untreated cells and those treated with H_2O_2 for 20 and 240 min. Samples were run on nine gels against a standard pool labelled with Cy2. A total of 138 significant changes were identified across the different conditions (>1.5-fold up- or down-regulated; $p < 0.05$). Of these, 117 were aligned to comigrating CCB-stained spots and 53 were identified by MALDI-MS with 30 displaying peroxide-dependence and 23 ErbB2-dependence, with 21 individual gene products in each group (Table 2 and Fig. 5D). As expected, there was some overlap with our previous work (7 out of 23 proteins), where the HB4a and C3.6 proteomes were compared by lysine labelling 2-D DIGE ([3] and unpublished data), and most of these protein isoforms displayed the same directionality of regulation in C3.6 *versus* HB4a cells, including MxA, Hsp70 protein 2, FK506-binding protein 4, L-plastin and cytokeratin 17 (Table 2B).

Although more differentially altered gel features could be matched between the studies, the moderate 'hit rates' for identifications meant that the overlap was not higher. Comparison between the ICy and NHS-Cy dye-labelling approaches revealed 18 common identities, representing isoforms of 11 individual gene products. In most cases, these displayed similar changes, indicating that the ICy dyes were detecting changes in abundance for these proteins. The identification of unique gene products in each set of experiments shows the usefulness of applying both techniques to better define the biological changes associated with H_2O_2 stress and ErbB2 overexpression. However, in the absence of a 100% hit rate for MS protein identification, it is difficult to compare the relative contributions of changes in abundance *versus* changes in thiol reactivity.

The differentially expressed proteins identified by NHS-Cy labelling and MS were again involved in redox regulation, protein folding, proliferative suppression, glycolysis and the cytoskeleton, suggesting that these cellular functions are the major targets of redox stress and ErbB2 overexpression. In addition, four citrate (TCA) cycle enzymes were modulated, including dihydrolipoamide dehydrogenase, which possesses a redox-active disulphide bond at its active site and four proteins involved in protein synthesis. Pxns1, 2, 3 and 6 were again identified, with Pxns1, 2 and 6 found in doublet spots of different p*I*s (Table 2A). Notably, the more basic spots in these doublets were down-regulated by H_2O_2 treatment, while the acidic spots were up-regulated. A similar pattern of regulation was reported in two previous studies, and was found to be due to oxidation of the active site cysteine thiols [20, 21]. These shifts help to explain the differential labelling by the ICy dyes (see above). Elongation factor 2 and enolase alpha also existed as multiple isoforms, where the more acidic isoforms were up-regulated by H_2O_2 treatment, suggesting that they too may be oxidised and shifted in p*I*. It is likely that such modifications would affect protein translation and glycolysis, respectively. There were also differences in the response of several proteins isoforms to H_2O_2 in the different cell lines, including Hsp73/71, Prxn6 and L-plastin (Table 2A); differences which reflect their altered abundance in the ErbB2 overexpressing cells (Table 2B). Together, these data show the complexity of the response of epithelial cells to redox stress and the effect that ErbB2 overexpression has on these responses.

4 Concluding remarks

In conclusion, we show that cysteine-labelling 2-D DIGE provides a MS-compatible and reproducible technique for identifying significant differences in the expression and redox modification of free thiol-containing proteins in multiple biological samples. This was achieved by labelling cysteine thiol groups with a matched pair of fluorescent alkylating agents at higher stoichiometry than that used with lysine amino groups in conventional 2-D DIGE. Although sample solubility is a problem when high stoichiometry labelling of either cysteine or lysine is carried out, we show that there is an analytical advantage to be gained from labelling the lower-occurrence cysteine residues: this is evident for example because heterogeneous labelling is reduced and redox-dependent thiol modifications can be simultaneously monitored. It is worth noting that our recent calculations predict that around 95% of all human ORFs encode a cysteine-containing protein (R. Jacobs, unpublished data). Although a proportion of these would not be accessible to alkylation, our data show significant labelling of free thiols in denatured, nonreduced lysates, with around 5% of the detectable proteins susceptible to changes in labelling in response to oxidative stress.

Table 2. Differentially expressed proteins identified by NHS-Cy 2-D DIGE and MS. (A) Proteins displaying H_2O_2-induced differential expression in HB4a and C3.6 HMLECs. (B) Proteins displaying differential expression between HB4a and C3.6 luminal epithelial cells. Proteins were identified by MALDI-TOF PMF (see Section 2). Annotations are as shown for Table 1

A

Spot no.	Protein name	% Cov.	Est. mass	Est. p/	Pred. Mass	Pred. p/	GI no.	Average fold-difference[b)] 4a(20') to 4a(0)	4a(240') to 4a(0)	3.6(20') to 3.6(0)	3.6(240') to 3.6(0')	Function
391	2-OGDH	31	110000	7.2	114601	8	1352618	-1.03	-1.15	1	-1.52	TCA cycle/oxidative metabolism
1123	Cytokeratin 6A	30	60000	8	59914	8.1	46812692	1.13	1.53	1.07	1.66	Cytoskeleton
1090	Dihydrolipoamide dehydrogenase	34	55000	7.8	54713	7.6	51095146	-1.09	-1.35	-1.11	-1.67	Regulation of cellular redox state
471	Elongation factor 2[a)]	25	95000	7.1	96246	6.4	119172	5.09	4.39	5.55	3.53	Protein synthesis
472	Elongation factor 2[a)]	26	95000	7.2	96246	6.4	119172	3.19	2.53	3.12	2.70	Protein synthesis
476	Elongation factor 2[a)]	41	95000	7.3	96246	6.4	119172	2.24	1.67	2.23	1.62	Protein synthesis
468	Elongation factor 2[a)]	29	95000	7.4	96246	6.4	119172	-1.34	-1.25	-1.5	-1.28	Protein synthesis
487	Elongation factor 2[a)]	37	95000	7.5	96246	6.4	119172	-2.48	-2.25	-3.27	-2.93	Protein synthesis
1345	Enolase alpha[a)]	41	47000	7.3	47481	7	29792061	1.34	1.46	1.52	1.94	Glycolysis
1347	Enolase alpha[a)]	76	47000	7.5	47481	7	29792061	-1.15	-1.59	-1.26	-1.82	Glycolysis
994	Hsp60 mitochondrial precursor	57	60000	5.5	61187	5.7	31542947	1.07	-1.07	-1.1	-1.89	Protein folding
764	Hsp70 protein 9B/mortalin-2[a)]	60	70000	6	73920	5.9	24234688	-1.09	-1.22	-1.11	-1.78	Protein folding
777	Hsp73/Hsp71[a)]	44	70000	5.6	73920	5.6	5729877	1.06	1.38	-1.01	1.7	Protein folding
713	Hsp73/Hsp71	60	70000	6.5	71082	5.7	5729877	1.19	1.57	-1.15	-1.20	Protein folding
1777	Lactate dehydrogenase B[a)]	56	37000	6	36801	5.7	49259212	-1.04	-1.4	-1.1	-1.74	Glycolysis (regeneration of NADH)
725	Lamin A/C[a)]	60	70000	8	70903	8.6	27436948	-1.58	-1.28	-1.43	-1.44	Nuclear envelope protein
863	L-plastin[a)]	60	70000	5.5	70815	5.2	4504965	-1.43	-1.34	-2.64	-1.40	Actin binding protein
503	NRAS-related protein	34	85000	6.5	80046	6.2	16356661	-1.03	-1.21	-1.03	-1.54	Ras oncoprotein family
2256	Peroxiredoxin 1[a)]	75	23000	8.5	22324	8.3	32455266	-4.91	-5.83	-6.54	-9.83	Protection from oxidative stress
2263	Peroxiredoxin 1[a)]	74	23000	8.3	22324	8.3	32455266	5.17	4.77	5.64	6.17	Protection from oxidative stress
2267	Peroxiredoxin 2 isoform b	25	20000	5.5	16036	6.1	33188452	11.71	9.38	8.57	8.80	Protection from oxidative stress
2264	Peroxiredoxin 2[a)]	63	22000	5.8	21892	5.7	2507169	-9	-4.14	-8.15	-7.39	Protection from oxidative stress
2211	Peroxiredoxin 3 isoform b	48	26000	7	25839	7	32483377	-4.03	-4.11	-3.04	-3.83	Protection from oxidative stress
2123	Peroxiredoxin 6[a)]	73	27000	6.2	25035	6	1718024	-1.85	-1.74	-1.41	-1.01	Protection from oxidative stress
2133	Peroxiredoxin 6[a)]	37	27000	6	25035	6	1718024	9.54	9.19	12.42	13.90	Protection from oxidative stress
2074	Phosphoglycerate mutase 1	53	28000	7	28931	6.8	49456447	-1.82	-1.73	-3.77	-3.97	Glycolysis
2076	Phosphomannomutase 2	28	28000	6.5	28406	6.4	4557839	-1.48	-1.51	-1.42	-1.55	Protein glycosylation
1352	Sorting nexin 5	28	47000	6.8	47072	6.3	23111047	1.19	2.08	1.26	2.50	Intracellular trafficking
762	TNFR1-associated protein/HSP 75	44	70000	8.3	70618	8	1082886	-1.13	-1.33	1.04	-2.11	Protein folding
503	UNR/Upstream of NRAS	31	85000	6.5	89684	5.9	12643993	-1.03	-1.21	-1.03	-1.54	RNA-binding/initiation of translation

B

Spot no.	Protein name	% Cov	Est. mass	Est. p/	Pred. Mass	Pred. p/	Accession no.	Average fold-difference[b)] 3.6 (0') to 4a(0')	3.6 (20') to 4a(20')	3.6 (240') to 4a(240')	Function
1202	Cytokeratin 13A	48	50000	5	49898	4.9	24234696	1.63	1.54	1.79	Cytoskeleton
1316	Cytokeratin 17[a)]	54	40000	5	40520	4.9	47939651	2.36	2.05	2.37	Cytoskeleton
1541	Cytokeratin 19	44	45000	4.8	44079	5	417200	-1.56	-1.6	-1.43	Cytoskeleton
1545	Cytokeratin 19[a)]	81	45000	4.9	44079	5	417200	-1.61	-1.82	-1.61	Cytoskeleton
1088	FK506-binding protein 4	35	52000	5.8	52057	5.4	4503729	-1.65	-1.51	-1.89	Immuno-regulation/protein folding (PPIase)
2221	Flavin reductase (NADPH)	53	24000	8	22219	7.1	32891807	-1.57	-1.29	-1.32	Protection from oxidative stress/iron metabolism
1406	Fumarate hydratase	43	50000	8.5	54773	8.8	32880021	1.63	1.63	1.5	TCA cycle enzyme
1294	Rb-binding protein p46[a)]	40	50000	5	48132	5.2	4506439	-1.73	-2.35	-3.41	Suppression of proliferation
2223	Glutathione *S*-transferase pi	25	25000	5.5	24678	5.7	121746	-1.94	-2.05	-1.84	Regulation of cellular redox state
800	HSP-70	52	70000	6	70263	5.6	32879973	-1.57	-1.77	-1.92	Protein folding
713	HSP-71	60	70000	6.5	71082	5.7	16741727	2.07	1.51	1.1	Protein folding
2366	Human eIF1[a)]	45	16000	5.5	16433	5.1	7546515	1.51	1.62	1.67	Protein synthesis
1688	Isocitrate dehydrogenase 3	26	40000	6.5	40022	6.5	5031777	1.67	1.63	1.31	TCA cycle enzyme
863	L-plastin[a)]	60	70000	5.5	70815	5.2	4504965	3.32	1.79	3.19	Actin bundling protein
592	Mito. inner memb. protein[a)]	33	85000	7	84026	6.1	12803209	1.5	1.47	1.33	Unknown
657	Myxovirus resistance protein 1	39	75000	6	75886	5.6	21619147	-4.88	-7.99	-6.86	Anti-viral protein/IFN-induced
668	Myxovirus resistance protein 1	55	75000	6.3	75886	5.6	21619147	-10.01	-6.7	-12.92	Anti-viral protein/IFN-induced
2211	Peroxiredoxin 3 isoform b	48	26000	7	25839	7	32483377	1.74	2.3	1.87	Cellular protection from oxidative stress
2123	Peroxiredoxin 6	73	27000	6.2	25035	6	1718024	-1.99	-1.51	-1.16	Cellular protection from oxidative stress
1025	Protein disulfide-isomerase	63	57000	4.8	57117	4.8	1085373	-1.51	-1.58	-1.41	Disulfide bond formation/protein folding
1411	Thioredoxin domain containing 4	28	45000	5	47297	5	37183214	-1.73	-2.21	-2.06	Protection from oxidative stress/protein folding
1134	Trp-tRNA synthetase isoform b	38	50000	6.3	48852	6	47419920	-1.67	-1.59	-1.7	Protein synthesis
1001	Ub-specific protease 14	37	60000	5.6	61317	5.6	30583205	-1.59	-1.68	-1.54	Unknown

Since free/reactive thiol groups play important roles in enzyme catalysis and protein function, their redox modification is likely to alter protein function or oxidant-dependent signal transduction. Given the importance of oxidative stress in disease, further studies should be undertaken to assess the functional significance of these modifications and to assess their role in cytoprotection, induced cellular damage and signalling.

The results of our study support the notion that ErbB2 overexpression has profound effects on the response of cells to oxidative stress through the regulated expression and activity of redox-sensitive enzymes and stress-inducible proteins. By the same token, there is growing evidence that generation of H_2O_2 and concurrent inhibition of protein tyrosine phosphatases is actually required for growth factor receptor-dependent tyrosine kinase signalling [40, 41]. Thus, ErbB2 signalling itself would be governed by the redox status of the cell. The up-regulation of RhoGDI1 in the ErbB2 overexpressing cells is interesting in this context (Table 1B), since in other cell systems it has been shown to modulate recruitment of the NADPH oxidase complex to Rho-family GTPases for superoxide ion generation [42]. It is tempting to speculate that this interaction also occurs in mammary luminal epithelial cells and may alter superoxide ion production and H_2O_2 levels. Moreover, our previous observation of the down-regulation of mitochondrial superoxide dismutase (MnSOD) in the C3.6 cells [3, 43] may also have impact on intracellular H_2O_2 levels. These changes may at least in part account for the altered H_2O_2-inducible activation of Erk1/2 and p38 MAPK signalling in this cell system (see above), which in turn has direct implications on the stress responses of normal *versus* tumour cells and the response to chemotherapy.

We would like to thank Dr. Ewald Schroder, Dr. Olah Judit and Dr. Dirk Gorlich for reagents. H-L.C. was funded by a UCL Graduate School Research Scholarship and a University Overseas Research Scholarship.

5 References

[1] Herbert, B. R., Harry, J. L., Packer, N. H., Gooley, A. A. *et al.*, *Trends Biotechnol.* 2001, *19*, S3–S9.

[2] Rabilloud, T., *Electrophoresis* 1994, *15*, 278–282.

[3] Gharbi, S., Gaffney, P., Yang, A., Zvelebil, M. J. *et al.*, *Mol. Cell. Proteomics* 2002, *1*, 91–98.

[4] Tonge, R., Shaw, J., Middleton, B., Rowlinson, R. *et al.*, *Proteomics* 2001, *1*, 377–396.

[5] Unlu, M., Morgan, M. E., Minden, J. S., *Electrophoresis* 1997, *18*, 2071–2077.

[6] Alban, A., David, S. O., Bjorkesten, L., Andersson, C. *et al.*, *Proteomics* 2003, *3*, 36–44.

[7] Shaw, J., Rowlinson, R., Nickson, J., Stone, T. *et al.*, *Proteomics* 2003, *3*, 1181–1195.

[8] Kondo, T., Seike, M., Mori, Y., Fujii, K. *et al.*, *Proteomics* 2003, *3*, 1758–1766.

[9] Evans, C. A., Tonge, R., Blinco, D., Pierce, A. *et al.*, *Blood* 2004, *103*, 3751–3759.

[10] Baty, J. W., Hampton, M. B., Winterbourn, C. C., *Proteomics* 2002, *2*, 1261–1266.

[11] Wu, Y., Kwon, K. S., Rhee, S. G., *FEBS Lett.* 1998, *440*, 111–115.

[12] Lee, S. R., Kwon, K. S., Kim, S. R., Rhee, S. G., *J. Biol. Chem.* 1998, *273*, 15366–15372.

[13] Maeda, K., Finnie, C., Svensson, B., *Biochem. J.* 2004, *378*, 497–507.

[14] Slamon, D. J., Clark, G. M., Wong, S. G., Levin, W. J. *et al.*, *Science* 1987, *235*, 177–182.

[15] Harris, R. A., Eichholtz, T. J., Hiles, I. D., Page, M. J. *et al.*, *Int. J. Cancer* 1999, *80*, 477–484.

[16] Shevchenko, A., Wilm, M., Vorm, O., Mann, M., *Anal. Chem.* 1996, *68*, 850–858.

[17] Neuhoff, V., Arold, N., Taube, D., Ehrhardt, W., *Electrophoresis* 1988, *9*, 255–262.

[18] Gorlich, D., Pante, N., Kutay, U., Aebi, U. *et al.*, *EMBO J.* 1996, *15*, 5584–5594.

[19] Galvani, M., Rovatti, L., Hamdan, M., Herbert, B. *et al.*, *Electrophoresis* 2001, *22*, 2066–2074.

[20] Rabilloud, T., Heller, M., Gasnier, F., Luche, S. *et al.*, *J. Biol. Chem.* 2002, *277*, 19396–19401.

[21] Wagner, E., Luche, S., Penna, L., Chevallet, M. *et al.*, *Biochem. J.* 2002, *366*, 777–785.

[22] Lee, S. P., Hwang, Y. S., Kim, Y. J., Kwon, K. S. *et al.*, *J. Biol. Chem.* 2001, *276*, 29826–29832.

[23] Lee, A. S., *Trends Biochem. Sci.* 2001, *26*, 504–510.

[24] Hung, C. C., Ichimura, T., Stevens, J. L., Bonventre, J. V., *J. Biol. Chem.* 2003, *278*, 29317–29326.

[25] Wood, Z. A., Schroder, E., Harris, J. R., Poole, L. B., *Trends Biochem. Sci.* 2003, *28*, 32–40.

[26] Godon, C., Lagniel, G., Lee, J., Buhler, J. M. *et al.*, *J. Biol. Chem.* 1998, *273*, 22480–22489.

[27] Shenton, D., Grant, C. M., *Biochem. J.* 2003, *374*, 513–519.

[28] McClung, J. K., Jupe, E. R., Liu, X. T., Dell'Orco, R. T., *Exp. Gerontol.* 1995, *30*, 99–124.

[29] Quimby, B. B., Dasso, M., *Curr. Opin. Cell. Biol.* 2003, *15*, 338–344.

[30] Connolly, T., Gilmore, R., *Cell* 1989, *57*, 599–610.

[31] Sarto, C., Binz, P. A., Mocarelli, P., *Electrophoresis* 2000, *21*, 1218–1226.

[32] Dalle-Donne, I., Rossi, R., Milzani, A., Di Simplicio, P. *et al.*, *Free Radic. Biol. Med.* 2001, *31*, 1624–1632.

[33] Huot, J., Houle, F., Spitz, D. R., Landry, J., *Cancer Res.* 1996, *56*, 273–279.

[34] Noh, D. Y., Ahn, S. J., Lee, R. A., Kim, S. W. *et al.*, *Anticancer Res.* 2001, *21*, 2085–2090.

[35] Shen, C., Nathan, C., *Mol. Med.* 2002, *8*, 95–102.

[36] Wonsey, D. R., Zeller, K. I., Dang, C. V., *Proc. Natl. Acad. Sci. USA* 2002, *99*, 6649–6654.

[37] Timms, J. F., White, S. L., O'Hare, M. J., Waterfield, M. D., *Oncogene* 2002, *21*, 6573–6586.

[38] Ferguson, A. T., Evron, E., Umbricht, C. B., Pandita, T. K. *et al.*, *Proc. Natl. Acad. Sci. USA* 2000, *97*, 6049–6054.

[39] Vercoutter-Edouart, A., Lemoine, J., Le Bourhis, X., Louis, H. *et al.*, *Cancer Res.* 2001, *61*, 76–80.

[40] Rhee, S. G., Bae, Y. S., Lee, S. R., Kwon, J., *Sci. STKE* 2000, *2000*, E1 1–6.

[41] Rhee, S. G., Chang, T. S., Bae, Y. S., Lee, S. R. *et al.*, *J. Am. Soc. Nephrol.* 2003, *14*, S211–S215.

[42] Olofsson, B., *Cell. Signal.* 1999, *11*, 545–554.

[43] White, S. L., Gharbi, S., Bertani, M. F., Chan, H. L. *et al.*, *Br. J. Cancer* 2004, *90*, 173–181.

